# Planar Substitutions to Lebesgue type Space-Filling Curves and Relatively Dense Fractal-like Sets in the Plane

J. Math. Anal. Appl. 530 (2024) 127654

Contents lists available at ScienceDirect

Journal of Mathematical Analysis and Applications

journal homepage: www.elsevier.com/locate/jmaa

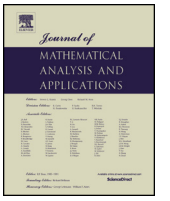

Regular Articles

# Planar substitutions to Lebesgue type space-filling curves and relatively dense fractal-like sets in the plane

Mustafa İsmail Özkaraca

*The Roslin Institute, The University of Edinburgh, Easter Bush Campus, EH25 9RG, Edinburgh, United Kingdom*

ARTICLE INFO

*Article history:*
Received 15 January 2023
Available online 18 August 2023
Submitted by A. Sims

*Keywords:*
Space-filling curves
Lebesgue curve
Fractal-like sets

ABSTRACT

We present an algorithm for generating curves filling the unit square; i.e. *space-filling curves*, from any given planar substitution satisfying a mild condition. The proposed algorithm is mimicking construction steps of *Lebesgue's curve* and is based on linear interpolation. Generated space-filling curves for some known substitutions are elucidated. Some of those substitutions further induce relatively dense fractal-like sets in the plane, whenever some additional assumptions are satisfied.



## 1. Introduction

A *space-filling curve* of the plane is a continuous mapping defined from the unit interval to a subset of the plane that has a positive area. The origin of space-filling curve theory goes back to late 1800s. Cantor proved in 1878 that there exists a bijective map between any pair of finite dimensional smooth manifolds [2]. Cantor's result was improved by Netto [9]. Netto showed in 1879 that such a map is necessarily discontinuous. Not being able to claim continuity and bijectivity simultaneously directed researchers to look for continuous surjections onto compact regions of the plane. Peano was first to discover a continuous map from the unit interval onto the unit square [10]. A year later, Hilbert constructed a space-filling curve through an infinite geometric iterative process [5]. Hilbert's curve is assumed to be the first space-filling curve that is built by a geometric construction because there was no hint of a geometric construction in Peano's approach.

Geometric interpretation of Hilbert's space-filling curve is usually presented by *approximating polygons/curves* (or *approximants* in short), a notion defined by Wunderlich [19]. There are numerous different versions of approximants of Hilbert's curve [15, P:23]. One version of the approximants is elucidated in Fig. 1. First approximant $\gamma_1 : [0,1] \mapsto [0,1] \times [0,1]$ is iterated to a curve $\gamma_2 : [0,1] \mapsto [0,1] \times [0,1]$ which is formed by concatenation of 4 scaled replicas (up to orientation) of the first approximant. Second approximant $\gamma_2$ is also substituted to third approximant $\gamma_3 : [0,1] \mapsto [0,1] \times [0,1]$ in the same fashion. This process

*E-mail address:* iozkarac@ed.ac.uk.

https://doi.org/10.1016/j.jmaa.2023.127654

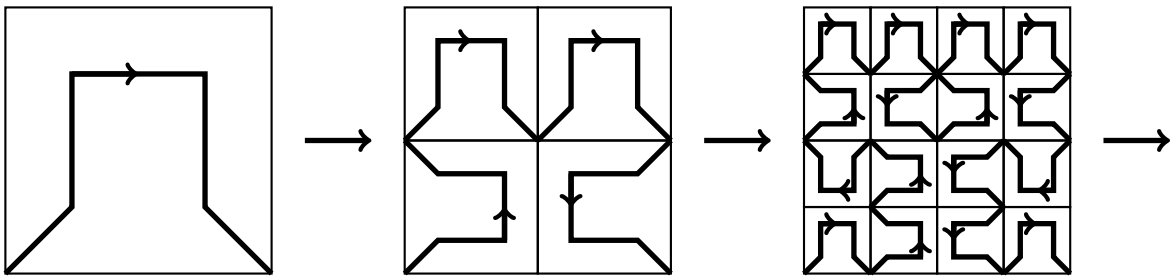

**Fig. 1.** First three approximating curves of Hilbert's curve.

continues ad infinitum. The sequence of approximants $\{\gamma_i : \ i \in \mathbb{Z}^+\}$ converges pointwisely to Hilbert's curve.

More examples of space-filling curves were given shortly after Hilbert [8,6,16,11], one of which was given by Lebesgue [6]. Unlike Hilbert's construction, Lebesgue defined a space-filling curve that is formed by linear interpolation over the map $\phi : \Gamma_c \mapsto [0,1] \times [0,1]$ given in (1.1), where $\Gamma_c$ is the middle-third Cantor set. The map $\phi$ is defined by ternary representations of points in the Cantor set, and is a continuous surjection onto the unit square.

$$\phi\left(0._3 \ (2\cdot x_1)(2\cdot x_2)(2\cdot x_3)\dots\right) = \begin{bmatrix} 0._2 \ x_1x_3x_5\dots, \\ 0._2 \ x_2x_4x_6\dots, \end{bmatrix}. \tag{1.1}$$

Geometric interpretation of Lebesgue's curve is clarified by Sagan [13,14]. Approximants of Lebesgue's curve are analogous to iteration steps of the Morton order, first three of which are depicted in Fig. 2. Using the approximants, Sagan provided another proof in his book [15], showing that Lebesgue's curve is a continuous surjection onto the unit square. This proof can be regarded as a geometric construction of Lebesgue's curve. In this study we generalise this construction.

A *tile* $t$ consists of a subset of $\mathbb{R}^n$ $(n \in \mathbb{Z}^+)$ and an assigned label. We denote the associated subset by supp $t$ and the label by $l(t)$. We assume that for every tile $t$, supp $t$ is homeomorphic to the closed unit disc. A *planar substitution* is a map defined over a collection of tiles in $\mathbb{R}^2$ such that it expands every tile by a fixed factor greater than 1, and divides each expanded tile into pieces, each of which is a translation of a tile. Throughout this paper we refer to planar substitutions as substitutions in short. In this document we introduce an algorithm producing space-filling curves from substitutions satisfying a weak condition, by mimicking the geometric construction of Lebesgue's curve. We also show that relatively dense sets in the plane (i.e. sets that have non-empty intersection with any ball $B(x,R)$ with centre $x \in \mathbb{R}^2$ and radius $R$, for some fixed $R > 0$) can be generated if some further conditions are satisfied. These sets also have fractal-like features in the sense that they can be dissected into countable pieces in which only finite number of them are distinct and others are congruent replicas of the distinct pieces.

The organisation of the paper is as follows. In Section 2, we provide relevant preliminary definitions and an example of a space-filling curve constructed through a substitution in detail. In Section 3, we define the space-filling curve generator algorithm (Theorem 3.1) and present examples of space-filling curves formed by this algorithm being applied over some of known substitutions (or their variations). Lastly, in Section 4, we explain and illustrate with an example how substitutions induce fractal-like sets that are relatively dense in $\mathbb{R}^2$.

## 2. Methodology

In this section we explain how to generalise the geometric construction of Lebesgue's curve with an example in detail.

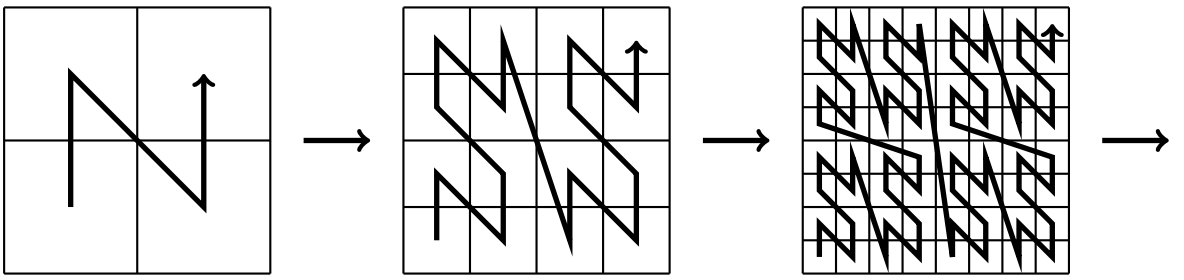

**Fig. 2.** First three iterations of the Morton order.

### 2.1. Substitutions

The material in this section is classical and can be found in textbooks such as [12].
Let $\mathbb{R}^2$ denote the Euclidean plane. We define the following:

1. A *tile* $t$ consists of a subset of $\mathbb{R}^2$ that is homeomorphic to the closed unit disc, and a label $l(t)$ that distinguishes $t$ from any other identical sets. The associated subset of $t$ is denoted by supp $t$. We call supp $t$ the *support* of $t$.
2. A *patch* $P$ is a finite collection of tiles so that
   (i) $\bigcup_{t\in P}$ supp $t$ is homeomorphic to the closed unit disc,
   (ii) int (supp $t$) $\cap$ int (supp $t'$) $= \emptyset$ for each distinct $t, t' \in P$.
   *Support of a patch* $P$ is union of supports of its tiles. It is denoted by supp $P$; i.e. supp $P = \bigcup_{t\in P}$ supp $t$.
3. For a given tile $t$, a vector $x \in \mathbb{R}^2$ and a non-zero scalar $\lambda \neq 0$, we create new tiles $t + x$ and $\lambda t$ by relations supp $(t+x) =$ (supp $t$) $+ x$, $l(t+x) = l(t)$, and supp $(\lambda t) = \lambda$supp $t$, $l(\lambda t) = l(t)$, respectively. We say $t+x$ is a *translation* of $t$ and $\lambda t$ is a *scaled copy* of $t$. Similarly, for a given patch $P$, a vector $x \in \mathbb{R}^2$ and a non-zero scalar $\lambda \neq 0$, we create new patches $P + x$ and $\lambda P$ by relations $P + x = \{t + x : \ t \in P\}$ and $\{\lambda t : \ t \in P\}$, respectively. We say $P + x$ is a *translation* of $P$ and $\lambda P$ is a *scaled copy* of $P$.

**Definition 2.1.** Suppose $\mathcal{P}$ is a given collection of tiles. Let $\mathcal{P}^*$ denote the set of all patches consisting of tiles that are translations of tiles in $\mathcal{P}$. A map $\omega : \mathcal{P} \mapsto \mathcal{P}^*$ is called a (*planar*) *substitution* if there exists $\lambda > 1$ such that supp $\omega(p) = \lambda \cdot$ supp $\omega(p)$ for all $p \in \mathcal{P}$.

We call $\lambda$ the *expansion factor* of $\omega$. We say that $\omega$ is a *finite substitution* if, in addition, $\mathcal{P}$ has a finite size.

**Definition 2.2.** For a given substitution $\omega : \mathcal{P} \mapsto \mathcal{P}^*$, the patch $\omega^n(p)$ for $p \in \mathcal{P}$ and $n \in \mathbb{Z}^+$ is called an *n-supertile* of $\omega$. It is also convenient to define that every tile in $\mathcal{P}$ is a 0-supertile of $\omega$; i.e. $\omega^0(p) := p$ for $p \in \mathcal{P}$.

An example of a substitution is given in Fig. 3. It is defined over two intervals $[0, (1+\sqrt{5})/2]$ and $[0, 1]$ with labels $a, b$, respectively. The interval $[0, (1+\sqrt{5})/2]$ with label $a$ is substituted into a patch consisting of two intervals $[0, (1+\sqrt{5})/2]$ and $[(1+\sqrt{5})/2, (3+\sqrt{5})/2]$ with labels $a, b$, respectively. The interval $[0, 1]$ with label $b$ is substituted into a patch consisting of a single interval $[0, (1+\sqrt{5})/2]$ with label $a$. This substitution is called the *Fibonacci substitution*. Expansion factor for the Fibonacci substitution is the golden mean $(1+\sqrt{5})/2$. By taking the Cartesian product of two Fibonacci substitutions, we get another substitution that is illustrated in Fig. 4. Throughout the document we denote the Fibonacci substitution by $\mu$, the Cartesian product of two Fibonacci substitutions by $\nu$ and their associated domains by $\mathcal{P}_\mu, \mathcal{P}_\nu$,

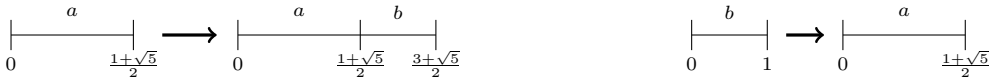


**Fig. 3.** The Fibonacci substitution $\mu$.

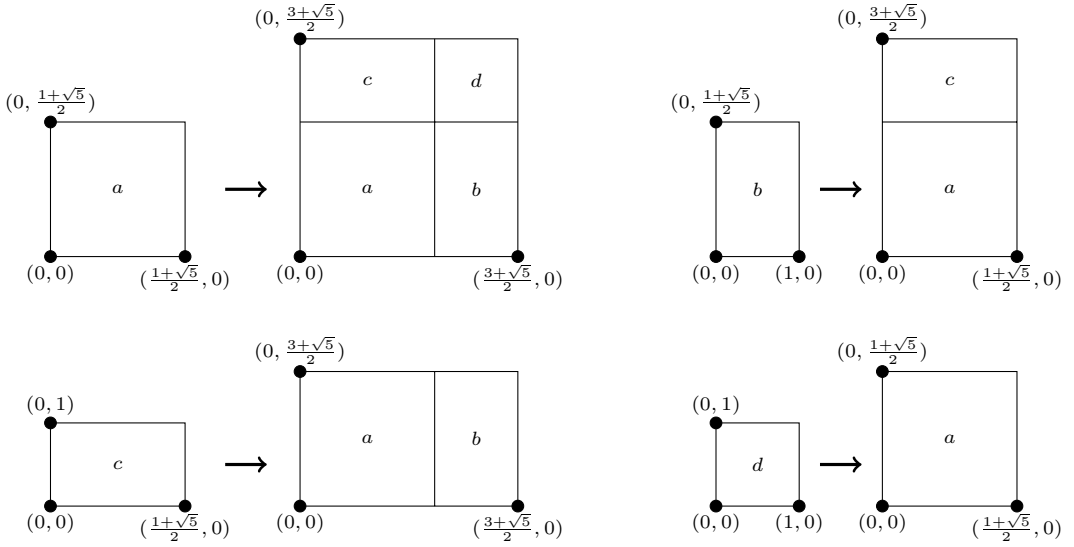


**Fig. 4.** The substitution $\nu$.

respectively. The domain $\mathcal{P}_\nu$ consists of four tiles $p_a, p_b, p_c, p_d$ such that $p_i$ is the tile with $l(p_i) = i$ for $i \in \{a, b, c, d\}$.

**Remark 2.3** *(Powers of substitutions).* Let $\omega : \mathcal{P} \mapsto \mathcal{P}^*$ be a given substitution with an expansion factor $\lambda$. Range of $\omega$ does not necessarily contain its domain and $\omega^2 = \omega \circ \omega$ may be ill-defined. Therefore, we define an extension $\omega' : \mathcal{P} + \mathbb{R}^2 \mapsto \mathcal{P}^*$ by $\omega'(p + x) = \omega(p) + \lambda \cdot x$ for $p \in \mathcal{P}$ and $x \in \mathbb{R}^2$, and define $(\omega')^n(p)$ for $p \in \mathcal{P}$ and $n \geq 2$ recursively as follows:

$$(\omega')^n(p) := \bigcup_{t \in (\omega')^{n-1}(p)} \omega'(t).$$

Powers of $(\omega')^n$ for $n \in \mathbb{Z}^+$ are well-defined. We use $\omega$ and $\omega'$ interchangeably, when there is no confusion of taking powers of substitutions.

### *2.2. Total order structures by $\nu$ through ordered Bratteli diagrams*

A fundamental ingredient of Sagan's geometric construction of Lebesgue's curve is approximating polygons [13,14]. For that, we define total orders over supertiles of $\nu$ using Bratteli diagrams [1,4]. These total order structures are key feature to form such approximating polygons. We start with defining basic terminology for Bratteli diagrams.

**Definition 2.4** *(Bratteli diagrams).* A directed graph $\mathcal{B} = (V, E)$ is called a Bratteli diagram if the vertex set $V$ and the edge set $E$ can be partitioned into infinite collection of mutually disjoint non-empty sets $\{V(i) : \ i = 0, 1, \dots\}$ and $\{E(i) : \ i = 1, \dots\}$ respectively such that

i. $V(0)$ is a singleton,

ii. There exist *range* $r : E \mapsto V$ and *source* $s : E \mapsto V$ maps so that $s^{-1}(v) \neq \emptyset$ for every $v \in V$ and $r^{-1}(v) \neq \emptyset$ for every $v \in V \backslash V(0)$.

The vertex at level-0 is called the *root vertex*.

Bratteli diagrams can be demonstrated by diagrammatic representation by levels $i = 0, 1, 2, \dots$ with $V(i)$ vertex set at level-$i$ and $E(i)$ edge set at level-$i$ with downward-oriented arrows connecting vertices between levels $i-1$ and $i$ for $i \in \mathbb{Z}^+$. In this document, we further assume that each vertex $v$ in a Bratteli diagram carries a label denoted by $l(v)$. An example of a diagrammatic representation of a Bratteli diagram is given in Fig. 5. Note that the diagram repeats after the first level. Such diagrams are called *stationary* Bratteli diagrams.

**Definition 2.5** *(Paths).* A *path* $P$ on a Bratteli diagram $\mathcal{B} = (E, V)$ is a collection of edges $\{e_i \in E : \ i = 1, \dots, n\}$ with $s(e_i) = r(e_{i-1})$ for each $i = 2, \dots, n-1$. We denote the path $P$ by $e_1 \circ e_2 \circ \cdots \circ e_n$. We assume that all paths are non-backtracking.

Range $r$ and source $s$ maps for edges can be extended for paths in a natural way. For any path $P = e_1 \circ \cdots \circ e_n$ on a Bratteli diagram $(V, E)$, we define *range* $r : P \mapsto V$ and *source* $s : P \mapsto V$ maps so that $r(P) := r(e_n)$ and $s(P) := s(e_1)$.

**Definition 2.6** *(Boundary of Bratteli diagrams).* The collection $\partial\mathcal{B}$ of all (non-backtracking) infinite paths starting at the root vertex of a Bratteli diagram $\mathcal{B}$ is a Cantor set under the product topology. We call $\partial\mathcal{B}$ the *boundary of* $\mathcal{B}$.

**Definition 2.7** *(Ancestors and descendants).* Let $v_1, v_2$ be two vertices in a Bratteli diagram $(V, E)$. Suppose there is a path $P$ with $s(P) = v_1$ and $r(P) = v_2$. We call $v_1$ an *ancestor* of $v_2$ with respect to $P$ and $v_2$ a *descendant* of $v_1$ with respect to $P$. If, in addition, there is an edge $e \in E$ so that $s(e) = v_1$ and $r(e) = v_2$, then we say $v_1$ is a *parent* of $v_2$ and $v_2$ is a *child* of $v_1$.

*Substitutions to Bratteli diagrams* A Bratteli diagram $\mathcal{B}_\omega = (V, E)$ can be constructed from a given substitution $\omega$ whenever vertices (which are endowed with labels) correspond to tiles in the substitution and an edge connecting vertices $a \in V(i-1)$ with $b \in V(i)$ indicates existence of a tile associated with vertex $b$ appearing in the substitution of a tile associated with vertex $a$. For example, the Bratteli diagram given in Fig. 5 is induced from the substitution $\nu$.

**Definition 2.8** *(Ordered Bratteli diagrams).* An *ordered Bratteli Diagram* is a Bratteli diagram $(V, E)$ with a partial order $\leq$ on $E$ such that every set $s^{-1}(\{v\})$ for $v \in V$ is totally ordered. It is denoted by $(V, E, \leq)$.

An example of an ordered (stationary) Bratteli diagram is shown in Fig. 6. It is the Bratteli diagram given in Fig. 5 with a partial order defined over its edges. The order structures between edges are apparent by the numbers attached to them, and repeat after the first level.

**Remark 2.9.** The usual construction of order structure for an ordered Bratteli diagrams is defined through pre-images of vertices by the range map. In this study, we rather use pre-images of vertices by the source map because we are interested in defining order structures on descendants of vertices.

**Definition 2.10.** Let $(V, E, \leq)$ be a given ordered Bratteli diagram. Suppose $S_{k,n}$ denote the set of all paths $P$ with $s(P) \in V(k)$ and $r(P) \in V(n)$ for some $k, n \in \mathbb{N}$ with $0 \leq k < n$. We define a (lexicographic) total order over $S_{k,n}$ as follows:

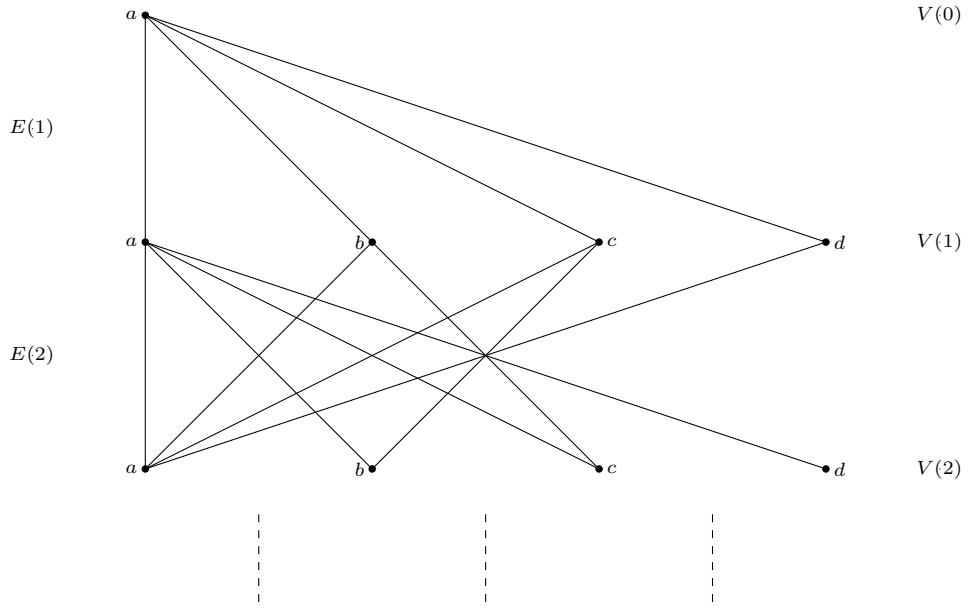


**Fig. 5.** A Bratteli diagram with $E(j+1) = E(2)$ and $V(j) = V(1)$ for all $j \in \mathbb{Z}^+$.

$$(e_{k+1}, e_{k+2}, \dots, e_n) < (f_{k+1}, f_{k+2}, \dots, f_n)$$

whenever $e_m < f_m$ for $m = \min\{i : e_i \neq f_i\}$, and $(e_{k+1}, e_{k+2}, \dots, e_n) = (f_{k+1}, f_{k+2}, \dots, f_n)$ whenever $e_i = f_i$ for all $i \in \{k+1, \dots, n\}$.

*Total orders induced by $\nu$* Paths in $S_{0,i}$ for the ordered Bratteli diagram shown in Fig. 6 correspond to tiles of $\nu^i(p_a)$ for every $i \in \mathbb{Z}^+$. As such, a lexicographic total order may be defined between tiles of $\nu^i(p_a)$ through total order between paths in $S_{0,i}$. For instance, total orders between tiles of 1-supertiles and 2-supertiles of $\nu$ are demonstrated in Fig. 7. Associated order structures are elucidated by the numbers attached to tiles in the figure.

*Partitions of the unit square by $\nu$* For every $k \in \mathbb{N}$, $\lambda^{-k-1} \cdot \nu^k(p_a)$ is a partition of the unit square with the convention that $\nu^0(p_a) := p_a$. The scaled patch $\lambda^{-k-1} \cdot \nu^k(p_a)$ consists of $\mathcal{F}^2_{k+2}$ rectangle tiles, where $\mathcal{F}_{k+2}$ is $(k+2)$-th Fibonacci number. Denote those tiles by $\mathcal{J}^1_k, \dots, \mathcal{J}^{\mathcal{F}^2_{k+2}}_k$ consecutively using total orders between supertiles of $\nu$. Then $\{\mathcal{J}^i_k : \ i = 1, \dots, \mathcal{F}^2_{k+2}\}$ is a partition of the unit square for each $k \in \mathbb{N}$. For example, $\{\mathcal{J}^1_0\}$, $\{\mathcal{J}^1_1, \dots, \mathcal{J}^4_1\}$ and $\{\mathcal{J}^1_2, \dots, \mathcal{J}^9_2\}$ are demonstrated in Fig. 8.

### *2.3. A construction of a Cantor set by $\nu$*

Consider the iteration rules shown in Fig. 9. The rules are defined for 4 different interval types of arbitrary length and demonstrate how to subdivide each interval type. Start with the interval $S_0 = [0, 1]$ attached with label $a$. Iterating it according to the given rules generates 4 subintervals with distinct labels $a, b, c, d$, respectively. Let $S_1$ denote the union of those 4 subintervals. For each generated subinterval, apply the rules in Fig. 9 and denote union of those subintervals as $S_2$, and so on so forth.

**Lemma 2.11.** *The set $\Gamma = \bigcap_{i=0}^{\infty} S_i$ is a Cantor set (i.e. totally disconnected, compact and perfect), when we ignore labels attached to $S_i$'s.*

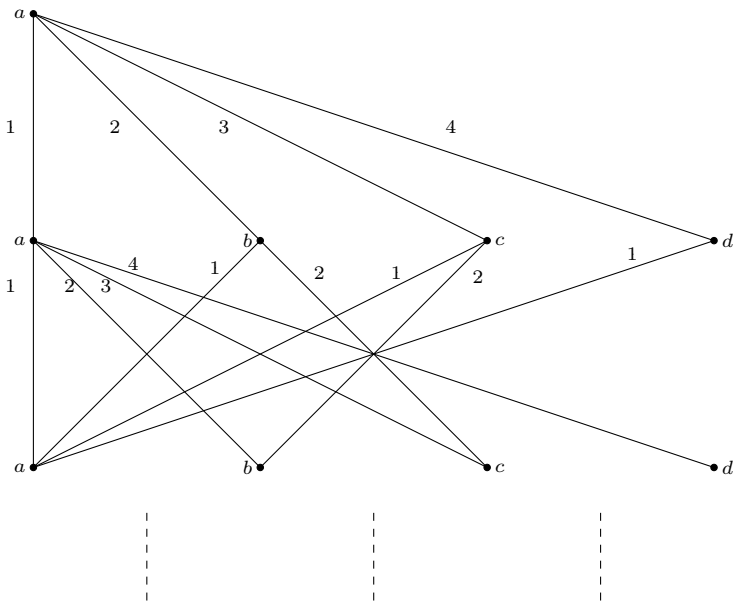


**Fig. 6.** An ordered Bratteli diagram with $E(j+1) = E(2)$ and $V(j) = V(1)$ for all $j \in \mathbb{Z}^+$.

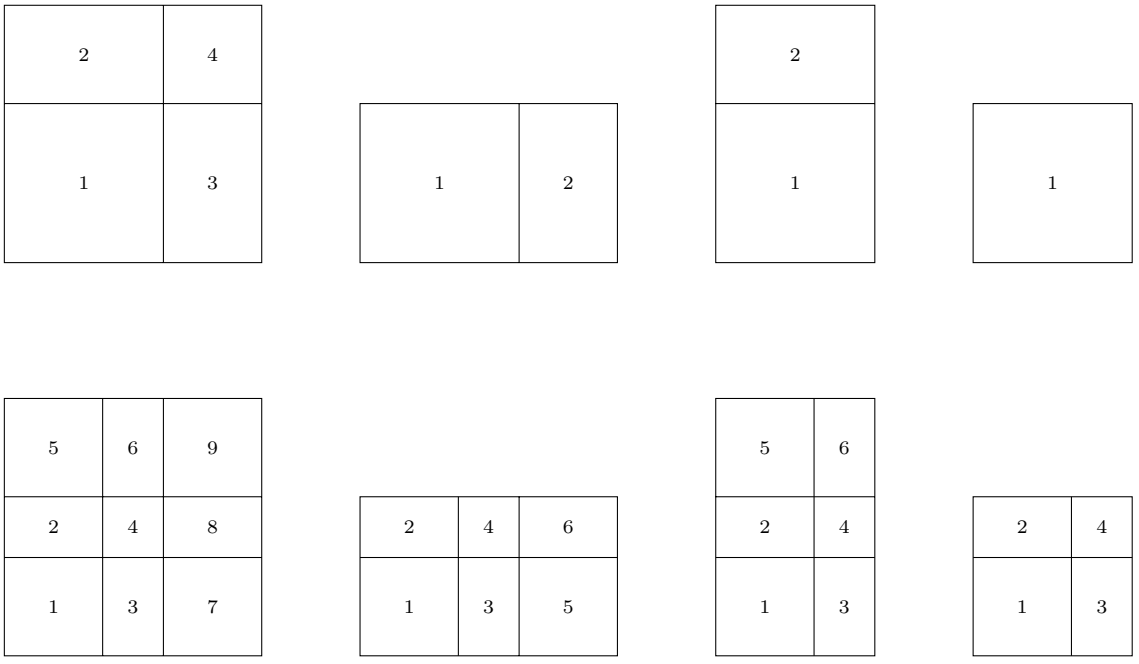


**Fig. 7.** The total orders between the tiles of 1-supertiles and 2-supertiles of $\nu$.

**Proof.** Proof follows by the fact that length of (disconnected) subintervals appearing in n-th step, for $n \in \mathbb{Z}^+$, decreases to zero as $n \to \infty$. □

First few steps of the construction of $\Gamma$ are shown in Fig. 10.

**Remark 2.12.** There is a natural correspondence between the boundary of the Bratteli diagram shown in Fig. 6, and $\Gamma$ in Lemma 2.11, where each infinite path in the diagram corresponds to a singleton in $\Gamma$. This

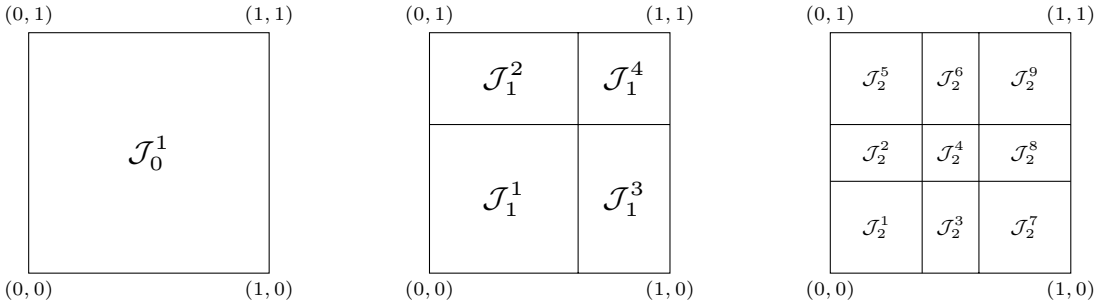


**Fig. 8.** A sequence of partitions of the unit square.

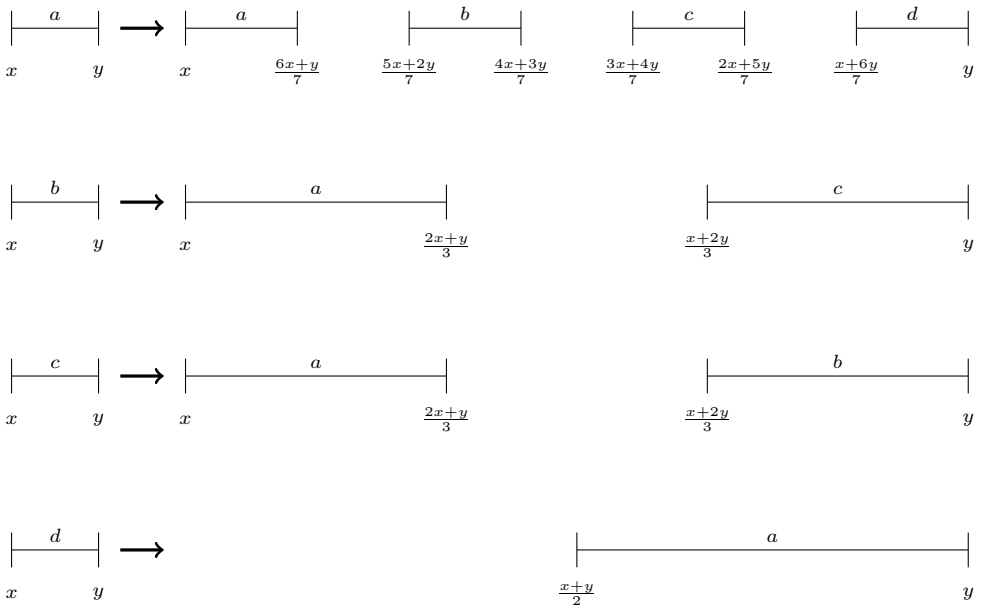


**Fig. 9.** An iteration rule.

can be seen whenever each vertex in the diagram is associated with a closed interval $[x, y] \subseteq [0, 1]$ with the help of iteration rules in Fig. 9 as follows:

i. The root vertex (which has a label $a$) is associated with $[0, 1]$.
ii. If a vertex has a label $a$ and is associated with $[x, y]$ then it has 4 children vertices with labels $a, b, c, d$ that are associated with intervals $\left[x, \frac{6x+y}{7}\right]$, $\left[\frac{5x+2y}{7}, \frac{4x+3y}{7}\right]$, $\left[\frac{3x+4y}{7}, \frac{2x+5y}{7}\right]$ and $\left[\frac{x+6y}{7}, y\right]$ respectively.
iii. If a vertex has a label $b$ and is associated with $[x, y]$ then it has 2 children vertices with labels $a, c$ that are associated with intervals $\left[x, \frac{2x+y}{3}\right]$ and $\left[\frac{x+2y}{3}, y\right]$ respectively.
iv. If a vertex has a label $c$ and is associated with $[x, y]$ then it has 2 children vertices with labels $a, b$ that are associated with intervals $\left[x, \frac{2x+y}{3}\right]$ and $\left[\frac{x+2y}{3}, y\right]$ respectively.
v. If a vertex has a label $d$ and is associated with $[x, y]$ then it has one child vertex with label $a$ that is associated with interval $\left[\frac{x+y}{2}, y\right]$.

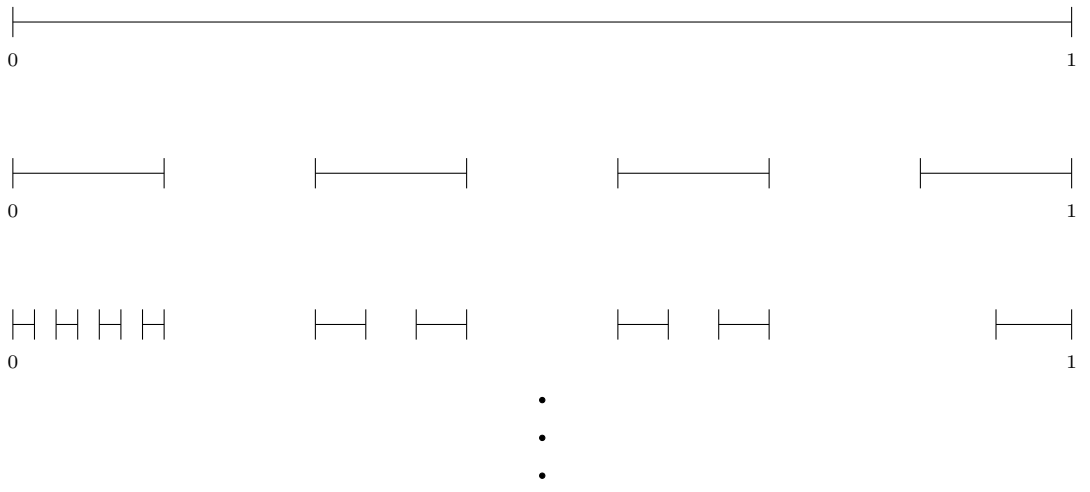


**Fig. 10.** Construction steps of Γ.

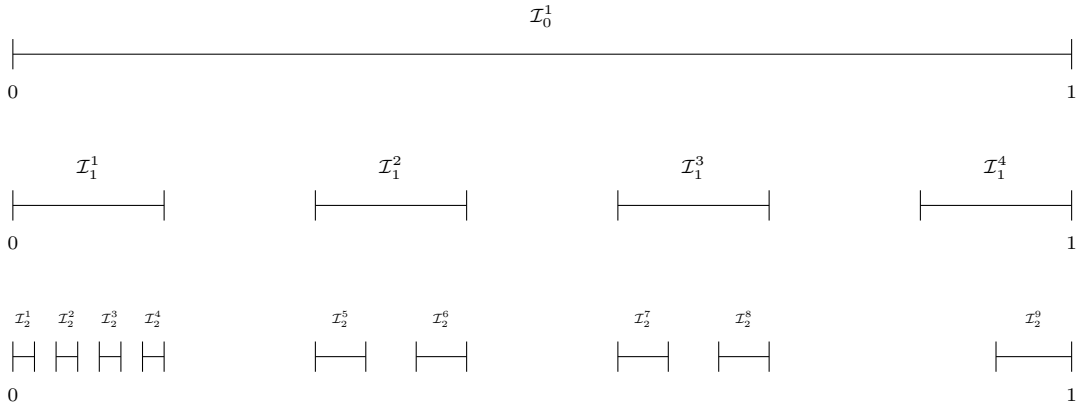


**Fig. 11.** Intervals $\mathcal{I}_0^1$, $\mathcal{I}_1^1, \ldots, \mathcal{I}_1^4$ and $\mathcal{I}_2^1, \ldots, \mathcal{I}_2^9$ are demonstrated.

An infinite path $P = e_1 \circ e_2 \circ \ldots$ passes through an infinite sequence of vertices $s(e_1), r(e_1), r(e_2), \ldots$ which corresponds to a sequence of closed intervals $I_1, I_2, \ldots$ with $\lim_{n\to\infty} I_n = 0$. Hence, $P$ can be identified with a unique singleton $\{x_P\} = \bigcap_{i=1}^{\infty} I_i$ by Cantor's intersection theorem.

### *2.4. A space-filling curve by ν*

Notice that there exist $\mathcal{F}_{k+2}^2$ many disjoint intervals in the n-th step (with the convention that [0,1] is the 0-th step) of construction of Γ, for every $n \in \mathbb{N}$. Denote these intervals by $\mathcal{I}_k^1, \ldots, \mathcal{I}_k^{\mathcal{F}_{k+2}^2}$, from left to right respectively. The intervals $\mathcal{I}_0^1$, $\mathcal{I}_1^1, \ldots, \mathcal{I}_1^4$ and $\mathcal{I}_2^1, \ldots, \mathcal{I}_2^9$ are demonstrated in Fig. 11.

For every $n \in \mathbb{N}$, $f_n : \{\mathcal{I}_n^k : \ k = 1, \ldots, \mathcal{F}_{n+2}^2\} \mapsto \{\mathcal{J}_n^k : \ k = 1, \ldots, \mathcal{F}_{n+2}^2\}$ defined by $f_n(\mathcal{I}_n^k) = \mathcal{J}_n^k$ for $k = 1, \ldots, \mathcal{F}_{n+2}^2$, is a bijection. Using this bijective correspondence, we define a space-filling curve as follows.

Let $x \in \Gamma$ be fixed. For every $n \in \mathbb{N}$, there exists a unique $k_n \in \{1, \ldots, \mathcal{F}_{n+2}^2\}$ such that $x \in \mathcal{I}_n^{k_n}$. In fact, $\{x\} = \bigcap_{n=1}^{\infty} \mathcal{I}_n^{k_n}$ by Cantor's intersection theorem. Similarly, $\bigcap_{n=1}^{\infty} \mathcal{J}_n^{k_n} = \{y\}$ for some unique $y \in [0,1] \times [0,1]$. Then $f : \Gamma \mapsto [0,1] \times [0,1]$ with $f(x) = y$ where $\{x\} = \bigcap_{n=1}^{\infty} \mathcal{I}_n^{k_n}$ and $\{y\} = \bigcap_{n=1}^{\infty} \mathcal{J}_n^{k_n}$ is well-defined.

**Theorem 2.13.** *The map $f : \Gamma \mapsto [0,1] \times [0,1]$ is a continuous surjection.*

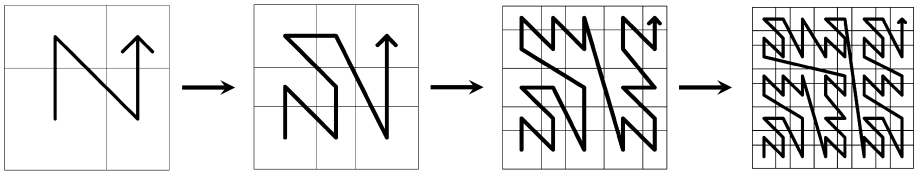

**Fig. 12.** First four approximants of $F$.

**Proof.** For any $y \in [0,1] \times [0,1]$, choose a sequence $m_n$ so that $\{y\} = \bigcap_{n=1}^{\infty} \mathcal{J}_n^{m_n}$. Note that such a sequence exists but not necessarily unique. Notice also that $\bigcap_{n=1}^{\infty} \mathcal{I}_n^{m_n}$ is a unique point. In fact, $f(\bigcap_{n=1}^{\infty} \mathcal{I}_n^{m_n}) = y$ and $f$ is a surjection. Next we prove $f$ is continuous.

For each $n \in \mathbb{Z}^+$, define the following:

$$g_n = \max_{j \in \{1,\dots,\mathcal{F}_{n+2}^2\}} \left\{ l(\mathcal{I}_n^j) : \ l(\mathcal{I}_n^j) \text{ denote length of } \mathcal{I}_n^j \right\},$$

$$h_n = \max_{j \in \{1,\dots,\mathcal{F}_{n+2}^2\}} \left\{ diam(\mathcal{J}_n^j) : \ diam(\mathcal{J}_n^j) \text{ denote diameter of } \mathcal{J}_n^j \right\}.$$

We have $g_n \downarrow 0$ and $h_n \downarrow 0$ as $n \to \infty$. Let $x \in \Gamma$ be fixed and let $\epsilon > 0$ be given. Choose $N \in \mathbb{Z}^+$ sufficiently large so that $h_N < \epsilon$. Set $\delta = g_N/2$. If $y \in \Gamma$ with $|x - y| < \delta$, then $x, y \in \mathcal{I}_N^{j_0}$ for some $j_0 \in \{1, \dots, \mathcal{F}_{N+2}^2\}$. That is, $f(x), f(y) \in \mathcal{J}_N^{j_0}$ and $||f(x) - f(y)|| < \epsilon$. Thus, $f$ is continuous. □

The continuous surjection $f : \Gamma \mapsto [0,1] \times [0,1]$ extends to a space-filling curve $F : [0,1] \mapsto [0,1] \times [0,1]$ by linear interpolation (See [13] for details of such process).

*A geometrisation of F* For each $n \in \mathbb{Z}^+$, mark the centre of every rectangle in $\lambda^{-n-1} \cdot \nu^n(p_a)$. Denote these points by $x(\mathcal{J}_n^j)$ for $j = 1, \dots, \mathcal{F}_{n+2}^2$. Join the points $x(\mathcal{J}_n^1), x(\mathcal{J}_n^2), \dots, x(\mathcal{J}_n^{\mathcal{F}_{n+2}^2})$ with straight lines, respectively. The constructed directed curve is called the *n-th approximant of F*. First four approximants of $F$ are shown in Fig. 12. (Fig. 13.)

## 3. A space-filling curve generator algorithm

In this section we generalise the argument presented in Section 2.

**Theorem 3.1.** *Let $\mathcal{P}$ be a given finite collection of tiles in $\mathbb{R}^2$. Suppose $\omega$ is a substitution defined over $\mathcal{P}$ such that* $\max\{diam(t) : \ t \in \lambda^{-n}\omega^n(p), \ p \in \mathcal{P}\} \downarrow 0$ *as $n \to \infty$, where $diam(t)$ denote diameter of* supp $t$ *and $\lambda$ denote expansion factor of $\omega$. Then for each $p \in \mathcal{P}$, there exists a Cantor set $\Gamma_{\omega,p} \subseteq [0,1]$ and a continuous surjection $f_{\omega,p} : \Gamma_{\omega,p} \mapsto$* supp $p$ *so that $f_{\omega,p}$ extends to a space-filling curve $F_{\omega,p} : [0,1] \mapsto$* supp $p$ *by linear interpolation.*

**Proof.** Let $\mathcal{P}$ be a finite collection of tiles. Suppose $\omega : \mathcal{P} \mapsto \mathcal{P}^*$ is a substitution with an expansion factor $\lambda > 1$ such that $\max\{diam(t) : \ t \in \lambda^{-n}\omega^n(q), \ q \in \mathcal{P}\} \downarrow 0$ as $n \to \infty$. Assume without loss of generality $|\omega(q)| > 1$ for all $q \in \mathcal{P}$.

Let $p \in \mathcal{P}$ be fixed. Define an ordered Bratteli diagram $\mathcal{B}_\omega = (V, E, \leq)$ from $\omega$ so that every vertex $v \in V$ is associated with $q_v \in \mathcal{P}$, the root vertex is associated with $p \in \mathcal{P}$ and every edge $e \in E$ indicates a copy of $q_{r(e)}$ appears in $\omega(q_{s(e)})$. Assume that $\{\mathcal{J}_{p,n}^k : \ k = 1, \dots, |\omega^n(p)|\}$ denotes the collection of rectangle tiles in $\lambda^{-n} \cdot \omega^n(p)$ for each $n \in \mathbb{N}$ such that

$$\mathcal{J}_{p,n}^1 < \mathcal{J}_{p,n}^2 < \cdots < \mathcal{J}_{p,n}^{|\omega^n(p)|}$$

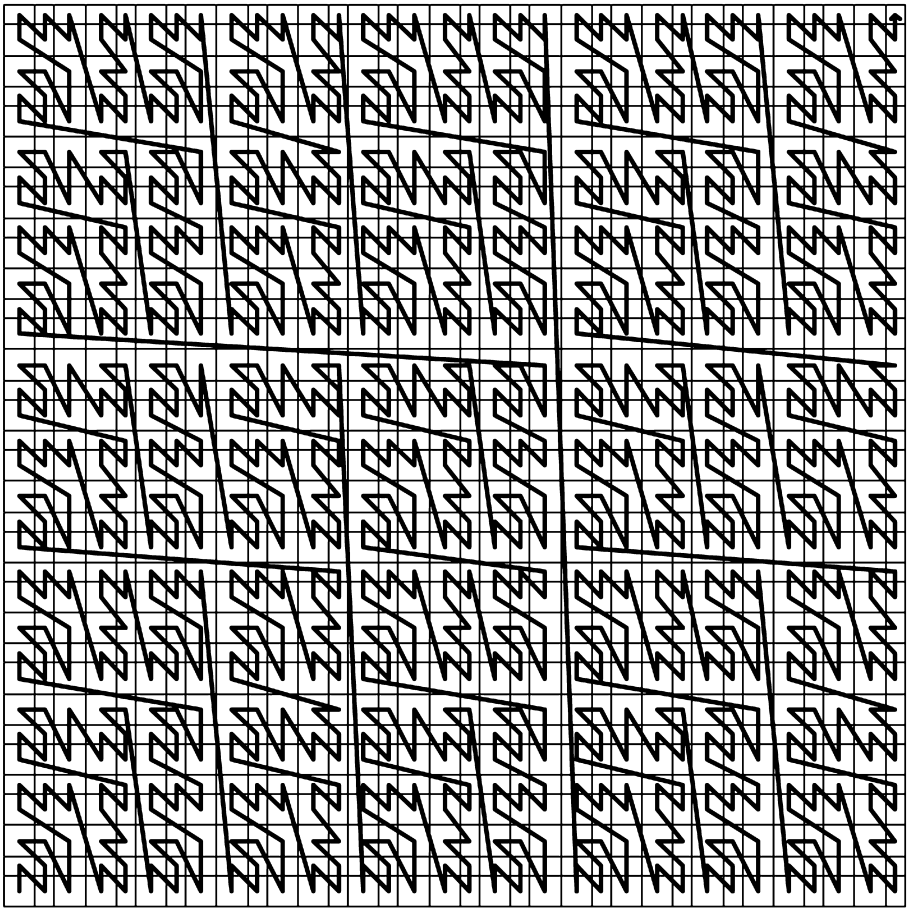

**Fig. 13.** 7th approximant of $F$.

with respect to order induced by $\mathcal{B}$.

The boundary $\partial\mathcal{B}_\omega$ is a Cantor set under the product topology. It can be embedded into a Cantor set $\Gamma_{\omega,p} \subseteq [0,1]$ whenever each infinite path is identified with a unique point in $[0,1]$ by associating every vertex $v \in V$ with a closed interval $[a,b]$ such that

i. The root vertex is associated with $[0,1]$
ii. If a vertex $v \in V$ is associated with $[a,b]$ and $e_1,\dots,e_r \in E$ are all edges with source $v$ so that $e_1 \leq e_2 \leq \cdots \leq e_r$ (with respect to $\mathcal{B}$), then vertex $r(e_i)$ is associated with subinterval $\left[a, a+(b-a)\dfrac{2i-1}{2r-1}\right]$ for $i = 1,2,\dots,r$.

Denote the intervals appearing in n-th step (with the convention that [0,1] is 0-th step) of construction of $\Gamma_{\omega,p}$ by $\mathcal{I}^1_{p,n},\dots,\mathcal{I}^{|\omega^n(p)|}_{p,n}$, from left to right respectively (as like in Fig. 11). For each $n \in \mathbb{Z}^+$, $f_{p,n} : \{\mathcal{I}^k_{p,n} : k = 1,\dots,|\omega^n(p)|\} \mapsto \{\mathcal{J}^k_{p,n} : \ k = 1,\dots,|\omega^n(p)|\}$ defined by $f_{p,n}(\mathcal{I}^k_{p,n}) = \mathcal{J}^k_{p,n}$ for $k = 1,\dots,|\omega^n(p)|$ is a well-defined bijection. For each $x \in \Gamma_{\omega,p}$ and $n \in \mathbb{N}$, there exists $k_{p,n} \in \{1,\dots,|\omega^n(p)|\}$ such that $x \in \mathcal{I}^{k_{p,n}}_{p,n}$. In particular, $\{x\} = \bigcap_{n=1}^{\infty} \mathcal{I}^{k_{p,n}}_{p,n}$ by Cantor's intersection theorem. By the same token, there exists $y \in \operatorname{supp} p$ such that $\{y\} = \bigcap_{n=1}^{\infty} \mathcal{J}^{k_{p,n}}_{p,n}$. This process induces a surjection $f_{\omega,p} : \Gamma_{\omega,p} \mapsto \operatorname{supp} p$ with $f_{\omega,p}(x) = y$ where $x$ and $y$ are as defined above. Next we prove that $f_{\omega,p}$ is continuous.

For each $n \in \mathbb{Z}^+$, define the following:

$$g_{p,n} = \max_{j\in\{1,\dots,|\omega^n(p)|\}} \left\{ l(\mathcal{I}^j_{p,n}) : \ l(\mathcal{I}^j_{p,n}) \text{ denote length of } \mathcal{I}^j_{p,n} \right\},$$

$$h_{p,n} = \max_{j\in\{1,\dots,|\omega^n(p)|\}} \left\{ diam(\mathcal{J}^j_{p,n}) : \ diam(\mathcal{J}^j_{p,n}) \text{ denote diameter of } \mathcal{J}^j_{p,n} \right\}.$$

We have that $g_{p,n} \downarrow 0$ and $h_{p,n} \downarrow 0$ as $n \to \infty$. Choose $x \in \Gamma_{\omega,p}$ and $\epsilon > 0$. Pick $N_p \in \mathbb{Z}^+$ sufficiently large so that $h_{p,N_p} < \epsilon$. Set $\delta = \frac{g_{p,N_p}}{2}$. If $y \in \Gamma_{\omega,p}$ with $|x-y| < \delta$, then $x, y \in \mathcal{I}^{j_0}_{p,N_p}$ for some $j_0 \in \{1,\dots,|\omega^{N_p}(p)|\}$. That is, $f(x), f(y) \in \mathcal{J}^{j_0}_{p,N_p}$ and $||f(x) - f(y)|| < \epsilon$. Thus, $f_{\omega,p}$ is continuous, and extends to a space-filling curve $F_{\omega,p} : [0,1] \mapsto \text{supp } p$ by linear interpolation. □

Theorem 3.1 can be regarded as an algorithm. Precisely, for every finite substitution $\omega : \mathcal{P} \mapsto \mathcal{P}^*$ satisfying the condition in Theorem 3.1 and a tile $p \in \mathcal{P}$, the following steps form a space-filling curve.

**Step − 1** : Choose $k \in \mathbb{Z}^+$ such that $|\omega^k(q)| > 1$ for every $q \in \mathcal{P}$.

**Remark 3.2.** Replace $\omega$ with $\omega^k$ for following steps. We assume without loss of generality $k = 1$ for the following steps.

**Step − 2** : Define an ordered Bratteli diagram $\mathcal{B}_\omega = (V, E, \leq)$ from $\omega$ with every vertex $v \in V$ is associated with $q_v \in \mathcal{P}$, the root vertex is associated with $p \in \mathcal{P}$ and every edge $e \in E$ indicates a copy of $q_{r(e)}$ appears in $\omega(q_{s(e)})$.

**Step − 3** : Define an order structure between scaled tiles in supertiles $\lambda^{-n} \cdot \omega^n(p)$ using $\mathcal{B}$.

**Step − 4** : Embed the Cantor set $\partial\mathcal{B}$ into $\Gamma_{\omega,p} \subseteq [0,1]$ by associating each infinite path with a distinct point in $[0,1]$.

**Step − 5** : Define a bijection between intervals appearing in the n-th construction step of $\Gamma_{\omega,p}$ and scaled tiles in $\lambda^{-n} \cdot \omega^n(p)$, for each $n \in \mathbb{Z}^+$.

**Step − 6** : Construct a continuous surjection $f_{\omega,p} : \Gamma_{\omega,p} \mapsto \text{supp } p$ using the bijective correspondences described in Step - 5.

**Step − 7** : Construct a space-filling curve $F_{\omega,p} : [0,1] \mapsto \text{supp } p$ by linear interpolation over $f_{\omega,p}$.

*The Vershik map* Proof of Theorem 3.1 would still hold even if $f_{p,n} : \Gamma_{\omega,p} \mapsto \text{supp } p$ would be replaced with $f_{p,n} \circ h : \Gamma_{\omega,p} \mapsto \text{supp } p$ for any homeomorphism $h : \Gamma_{\omega,p} \mapsto \Gamma_{\omega,p}$. In particular, interpolation of $f_{p,n} \circ h$ generates a (different) space-filling curve which is a deformation of the original. The *Vershik map* is a homeomorphism on the boundary of an ordered Bratteli diagram, whenever the diagram satisfies some mild conditions, and is conjugate to shifting a sequence by 1 whenever infinite paths are encoded as infinite sequences using lexicographic order structure induced from the Bratteli diagram [17,18]. In this paper, we have not studied deformations of constructed space-filling curves by the Vershik map, because their geometric interpretations are not obvious.

### *3.1. Space-filling curve examples*

In Section 3.1 we apply the algorithm induced from Theorem 3.1 using some of known substitutions. The substitutions provided in this section, as well as a vast collection of other substitutions, can be found in [3]. The generated space-filling curves are elucidated by their associated approximants (Definition 3.3).

**Definition 3.3.** Let $F_{\omega,p}$ be a space-filling curve constructed by the algorithm in Section 3. With the same notations in the proof of Theorem 3.1, for each $n \in \mathbb{Z}^+$ and $j \in \{1,\dots,|\omega^n(p)|\}$, denote the centre of $\mathcal{J}^j_{p,n}$ by $x(\mathcal{J}^j_{p.n})$. The directed curve formed by joining points $x(\mathcal{J}^1_{p.n}), x(\mathcal{J}^2_{p.n}), \dots, x(\mathcal{J}^{|\omega^n(p)|}_{p.n})$ successively is called *n-th approximant of* $F_{\omega,p}$.

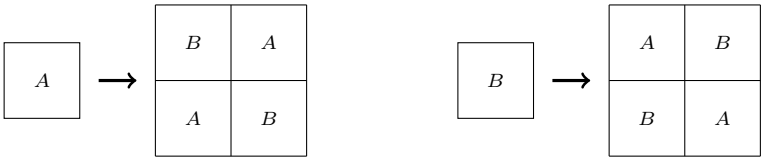


**Fig. 14.** 2-dimensional Thue-Morse substitution.

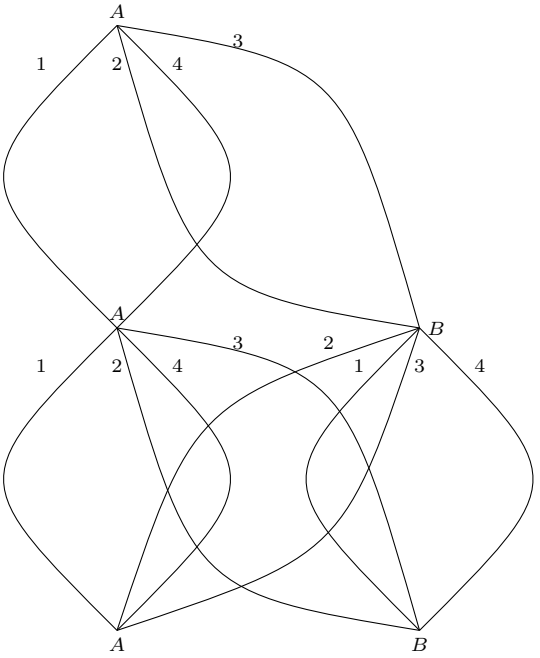


**Fig. 15.** An ordered stationary Bratteli diagram induced from 2-dimensional Thue-Morse substitution. Only level-0 and level-1 are presented.

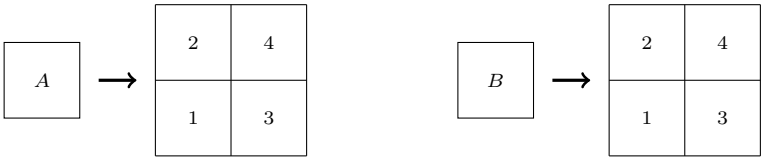


**Fig. 16.** Total orders over 1-supertiles of 2DTM.

**Example 3.4** *(Thue-Morse).* The substitution given in Fig. 14 is called *2-dimensional Thue-Morse substitution* (2DTM in short). It is defined over two unit squares with labels $A, B$. Expansion factor for this substitution is 2. Choose a square tile with label $A$ in order to input it to the algorithm.

Fig. 15 shows an ordered (stationary) Bratteli diagram defined from Thue-Morse substitution. Tiles between 1-supertiles of 2DTM can be totally ordered using the order structure of the diagram, as elucidated by numbers in Fig. 16. This can also be represented by curves depicted in Fig. 17 where the total order is defined according to which tile is visited first by the curve. The space-filling curve generated by the algorithm is nothing but the Lebesgue's curve.

Hereafter, we explain total order structures solely through directed curves (as like in Fig. 17) and bypass the step of defining ordered Bratteli diagrams. The associated total orders are defined according to which tile is visited first.

Next define another order structure over 1-supertiles of 2DTM by the curves shown in Fig. 18. Let $F^A_{tm}$ denote the space-filling curve formed by the algorithm (by inputting a tile with label $A$). First four

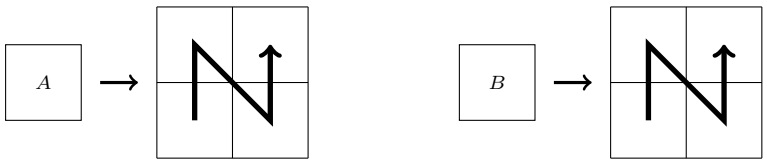


**Fig. 17.** Total orders defined through curves for the 1-supertiles of 2DTM.

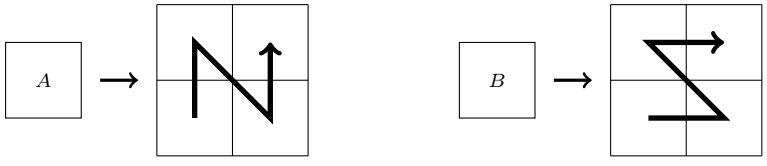


**Fig. 18.** Total orders over 1-supertiles of 2DTM.

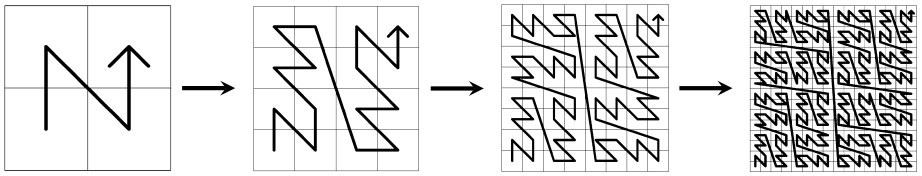

**Fig. 19.** First four approximants of $F^A_{tm}$.

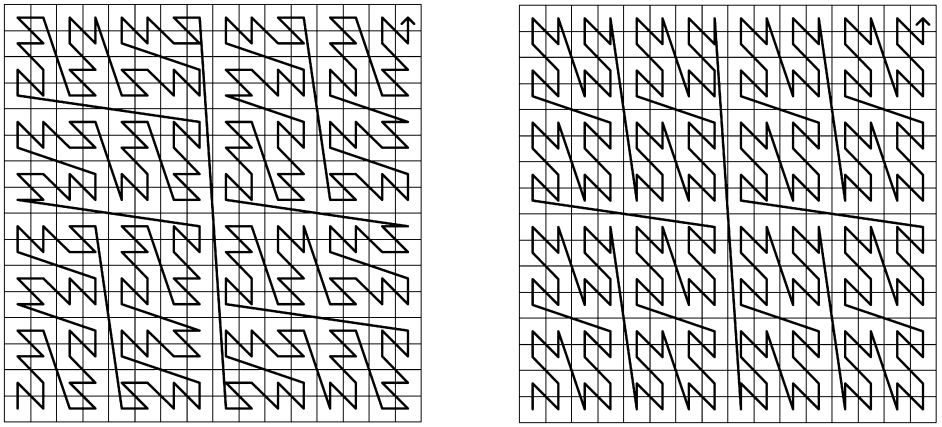

**Fig. 20.** 4th approximants of $F^A_{tm}$ and Lebesgue's curve, respectively.

approximants of $F^A_{tm}$ are shown in Fig. 19. Comparison of 4th approximants of $F^A_{tm}$ and the Lebesgue's curve is shown in Fig. 20.

**Example 3.5** *(Equithirds-variant).* Consider the substitution depicted in Fig. 21. It is a variation of *Equithirds substitution* [3]. It is defined over two different shapes; an equilateral triangle with side length 1 and an isosceles triangle with side lengths $1, 1, \sqrt{3}$. Its expansion factor is $\sqrt{3}$. The curves shown in Fig. 22 describe total orders over its 1-supertiles. Let $F^i_{eq}$ denote the space-filling curve produced by the algorithm from tile with label $i$ for $i \in \{A^+, A^-, B^+, B^-\}$. First four approximants of $F^{B^+}_{eq}$ are shown in Fig. 23. We modify approximants of $F^{B^+}_{eq}$ to be closed curves for demonstration purposes, by connecting end points of its approximants with a straight line and fill associated closed regions as illustrated in Fig. 24 and Fig. 25.

Next we describe geometry of approximants of $F^{A^+}_{eq}$. First four approximants of $F^{B^+}_{eq}$ are shown in Fig. 26. Notice that $F^{A^+}_{eq}(0) \neq F^{A^+}_{eq}(1)$. Let $p^r_{A^+}$ denote rotation of $p_{A^+}$ by $\pi$ such that longer edges of $p_{A^+}$ and $p^r_{A^+}$ merge. Suppose $F^{A^+_r}_{eq}$ is the space-filling curve generated by the algorithm using $p^r_{A^+}$. Since $F^{A^+}_{eq}(0) = F^{A^+_r}_{eq}(1)$

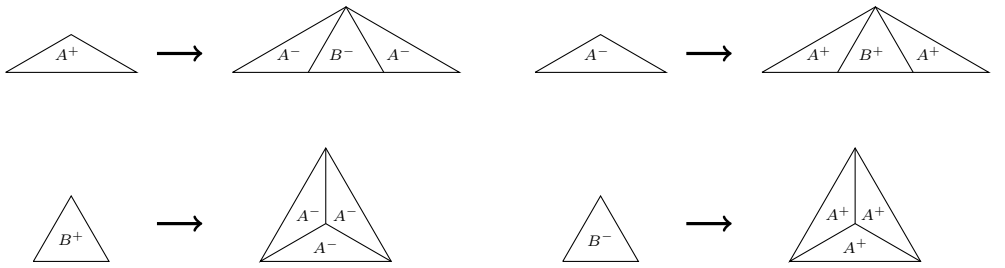


**Fig. 21.** Equithirds-variant.

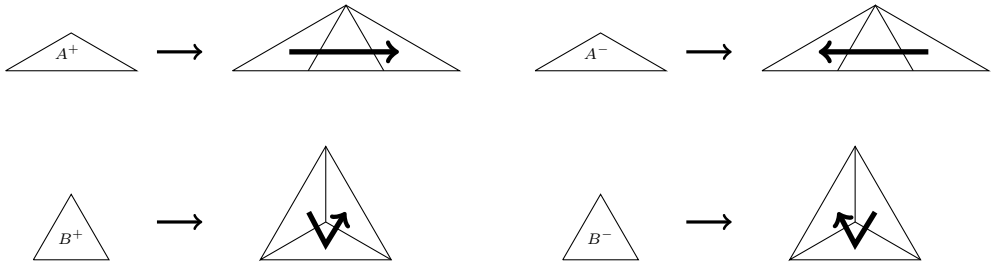


**Fig. 22.** Total orders over the 1-supertiles of Equithirds-variant.

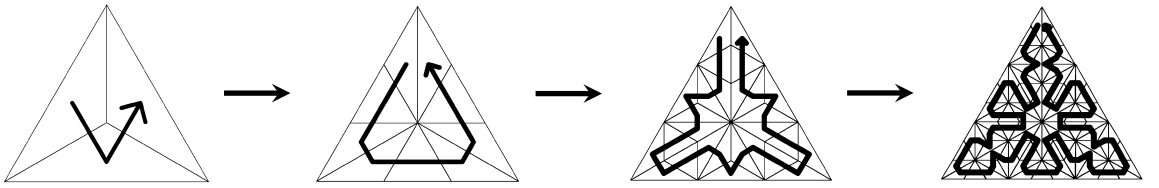

**Fig. 23.** First four approximants of $F_{eq}^{B^+}$.

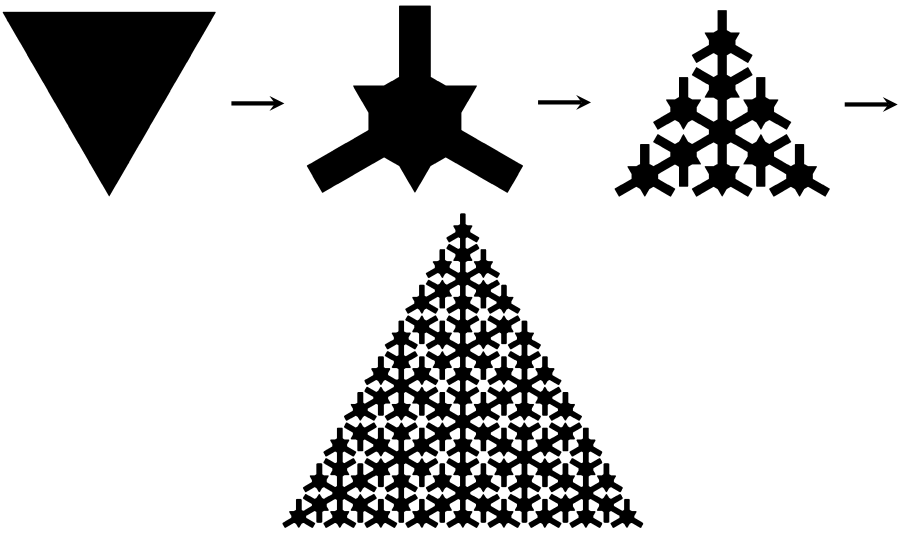

**Fig. 24.** 1st, 3rd, 5th and 7th approximants of $F_{eq}^{B^+}$. The 7th approximant is scaled up for illustration purposes.

and $F_{eq}^{A^+}(1) = F_{eq}^{A_r^+}(0)$, we can concatenate $F_{eq}^{A^+}$ with $F_{eq}^{A_r^+}$ in order to define another space-filling curve $F_{eq}^{A}$ with $F_{eq}^{A}(0) = F_{eq}^{A}(1)$. Approximants of $F_{eq}^{A^+}$ will be visualised through approximants of $F_{eq}^{A}$ because we can modify the approximants of $F_{eq}^{A}$ to be closed curves as shown in Fig. 27. Associated filled regions of first 8 approximant curves are shown in Fig. 28 and Fig. 29.

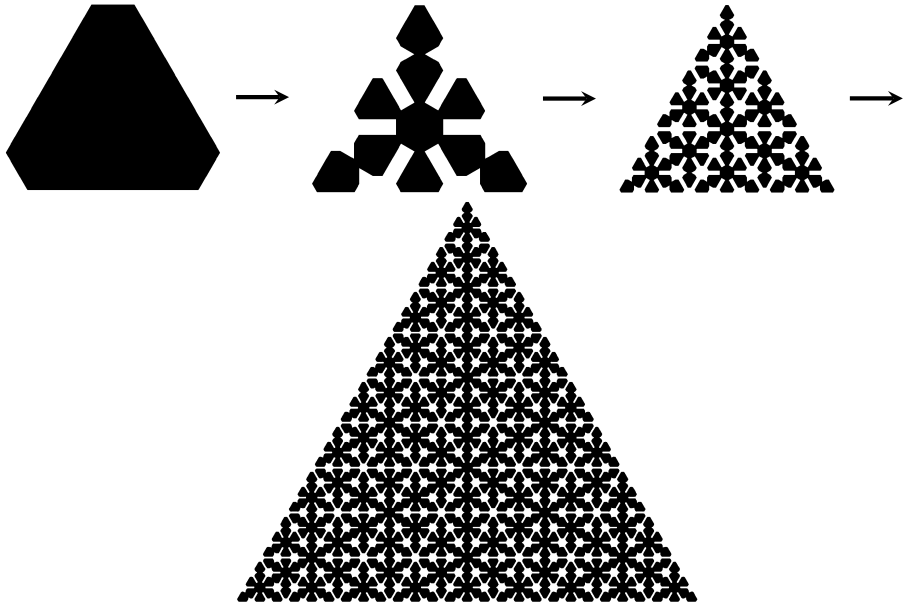

**Fig. 25.** 2nd, 4th, 6th and 8th approximants of $F_{eq}^{B^+}$. The 8th approximant is scaled up for illustration purposes.

**Fig. 26.** First four approximants of $F_{eq}^{A^+}$.

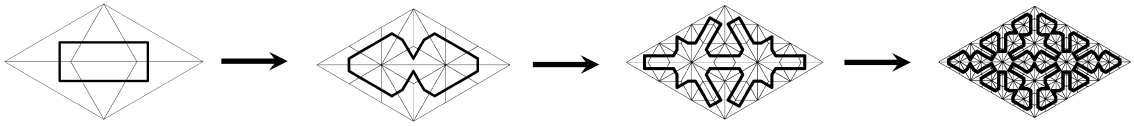

**Fig. 27.** First four approximants of $F_{eq}^{A}$ where their end points are joined with a line.

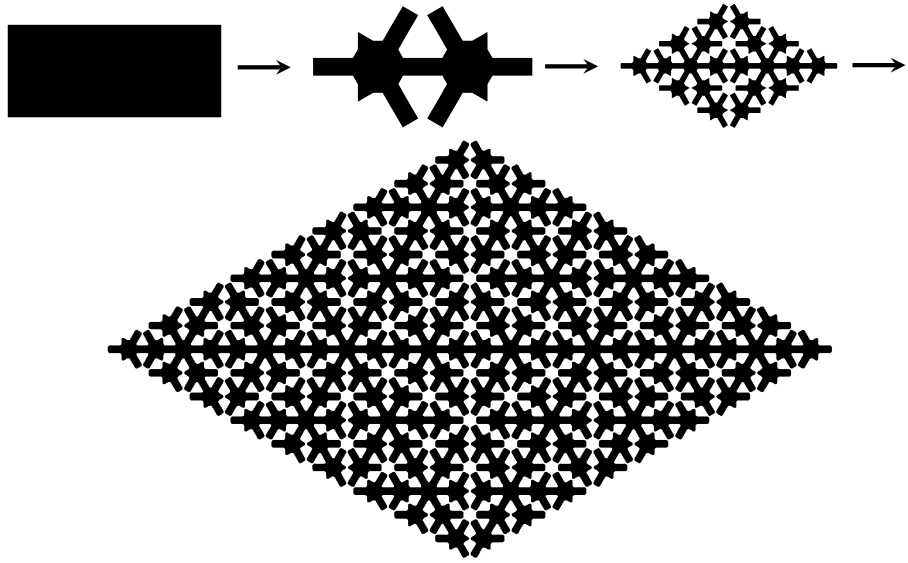

**Fig. 28.** Filled versions of 1st, 3rd, 5th and 7th approximants of $F_{eq}^{A}$. The 7th approximant is scaled up for demonstration purposes.

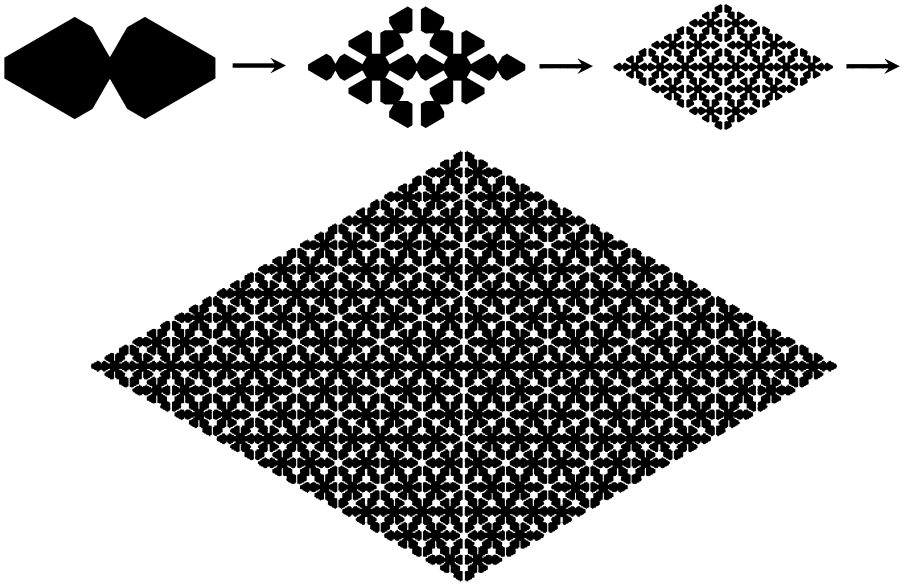

**Fig. 29.** Filled versions of 2nd, 4th, 6th and 8th approximants of $F^A_{eq}$. The 8th approximant is scaled up for demonstration purposes.

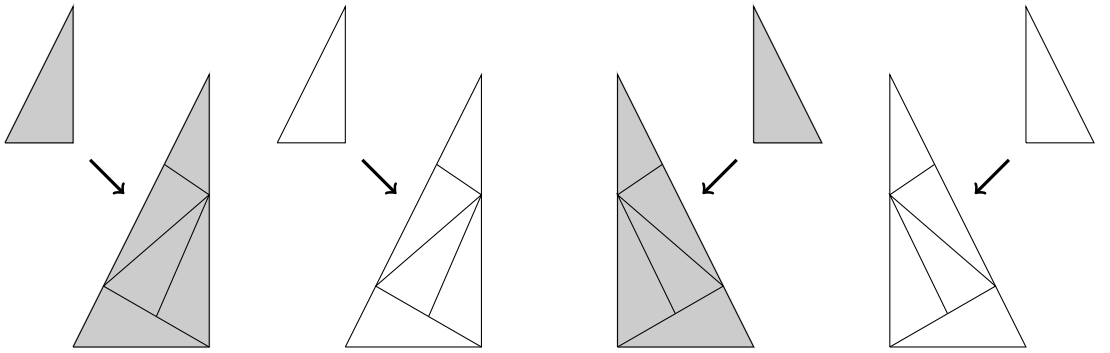

**Fig. 30.** Pinwheel-variant substitution.

For the following two substitution examples, we will use the algorithm (Theorem 3.1) to create space-filling curves over patches instead of tiles, similar to construction of $F^A_{eq}$, for demonstration purposes.

**Example 3.6** *(Pinwheel-variant).* The substitution given in Fig. 30 is defined over four tiles and their rotations. It is a variation of *Pinwheel substitution* [3]. Every tile in the substitution is a right triangle with side lengths $1, 2, \sqrt{5}$. Expansion factor for this substitution is $\sqrt{5}$. The curves in Fig. 31 define total orders over 1-supertiles of this substitution. Let $R_1, R_2$ denote rhombus and rectangle shown in Fig. 32. Using the algorithm together with the defined total orders, we can produce two space-filling curves $F^1_{pin}, F^2_{pin}$ over $R_1, R_2$, respectively. Fig. 33 indicates the first two approximants of $F^1_{pin}$ and $F^2_{pin}$. Observe that $F^i_{pin}(0) = F^i_{pin}(1)$ for $i = 1, 2$. Fig. 34 and Fig. 35 demonstrates first 5 approximants of $F^1_{pin}$, whereas Fig. 36 and Fig. 37 illustrates first 6 approximants of $F^2_{pin}$.

**Example 3.7** *(Penrose-Robinson-variant).* Start with the substitution given in Fig. 38. Its domain consists of 12 tiles and their rotations, which are congruent copy of two different shapes; an isosceles triangle with side lengths $1, 1, (1+\sqrt{5})/2$ and an isosceles triangle with side lengths $1, 1, (\sqrt{5}-1)/2$. Expansion factor for this substitution is the golden mean $(1+\sqrt{5})/2$. It is a variation of *Penrose-Robinson substitution* [3]. We generate space-filling curves $F_{star}, F_{deca}$ using the described total orders in Fig. 39. They fill supports of the

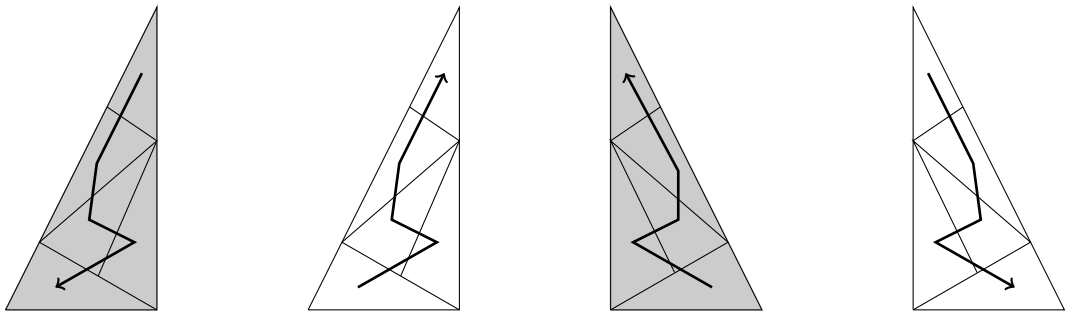

**Fig. 31.** Total orders over 1-supertiles of the Pinwheel-variant substitution.

**Fig. 32.** The regions $R_1$ and $R_2$, from left to right respectively.

**Fig. 33.** First two approximants of $F^1_{pin}$ and $F^2_{pin}$.

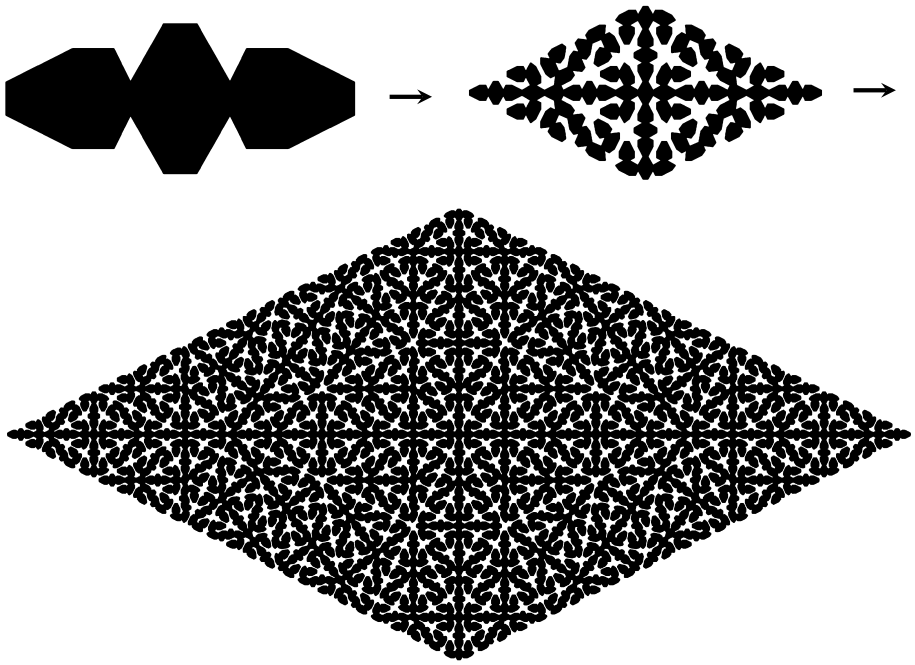

**Fig. 34.** 1st, 3rd and 5th approximants of $F^1_{pin}$ - filled version. The 5th approximant is scaled up for illustration purposes.

patches shown in Fig. 40, respectively, such that $F_{star}(0) = F_{star}(1)$ and $F_{deca}(0) = F_{deca}(1)$. Approximants of $F_{star}$ and $F_{deca}$ are shown in Fig. 41, Fig. 42 and Fig. 43.

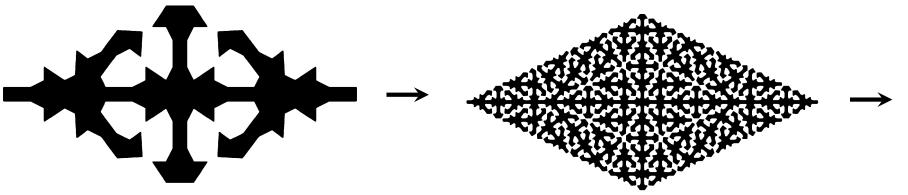

**Fig. 35.** 2nd and 4th approximants of $F^1_{pin}$ - filled version.

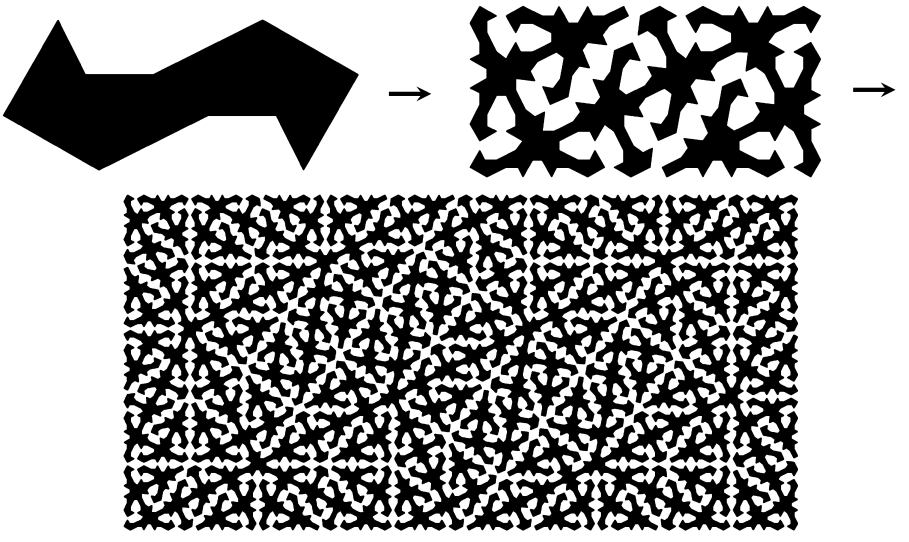

**Fig. 36.** 1st, 3rd and 5th approximants of $F^2_{pin}$ - filled version. The 5th approximant is scaled up for illustration purposes.

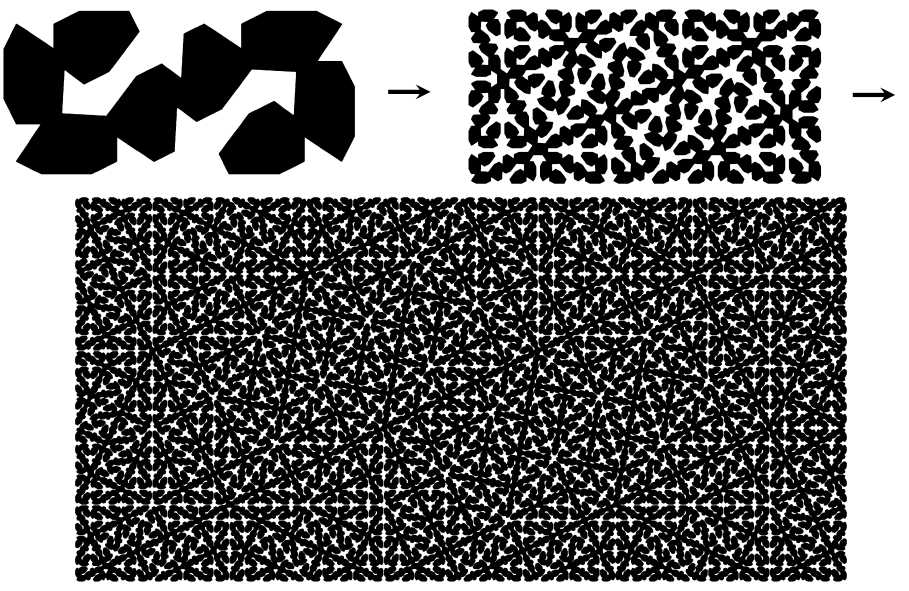

**Fig. 37.** 2nd, 4th and 6th approximants of $F^2_{pin}$ - filled version. The 6th approximant is scaled up for illustration purposes.

## 4. Substitutions to fractal-like relatively dense sets

**Definition 4.1.** A substitution $\omega : \mathcal{P} \mapsto \mathcal{P}^*$ is called *primitive* if there exists $k \in \mathbb{Z}^+$ such that $\omega^k(p)$ contains a copy of $q$ for every $p, q \in \mathcal{P}$.

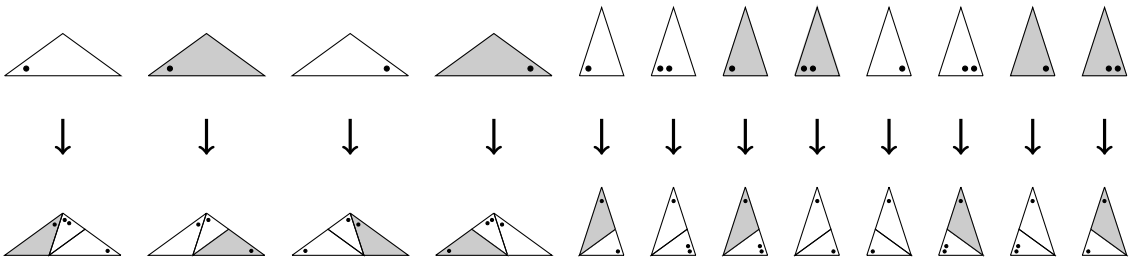

**Fig. 38.** Penrose-Robinson-variant substitution. 1-supertiles are scaled down for demonstration.

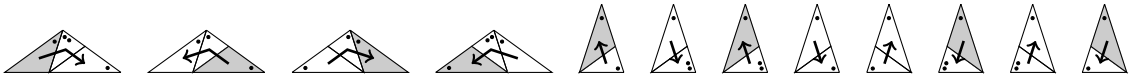

**Fig. 39.** Total orders over 1-supertiles of the Penrose-Robinson-variant substitution.

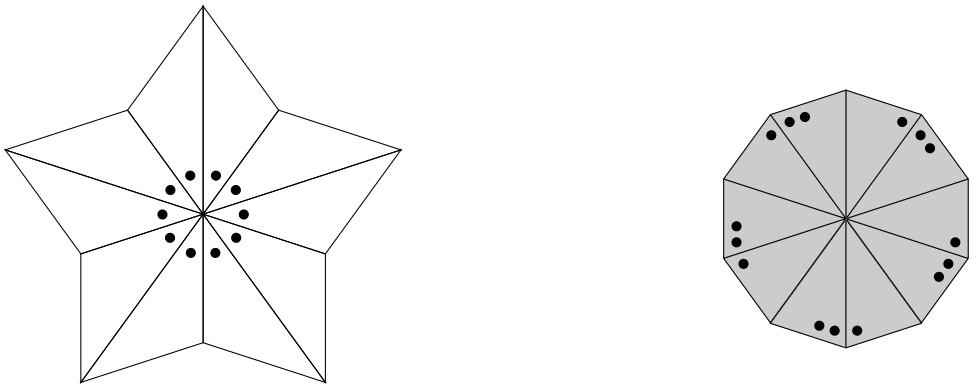

**Fig. 40.** A star and a decagon.

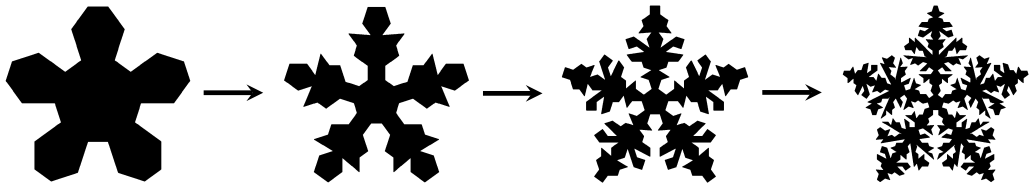

**Fig. 41.** First four approximants of $F_{star}$ - filled version.

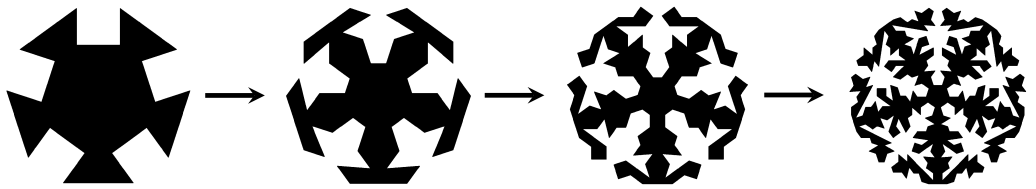

**Fig. 42.** First four approximants of $F_{deca}$ - filled version.

Primitive substitutions induce tessellations of the plane, called *tilings*.

**Definition 4.2** *(Tilings).* A tiling $T$ is a countable collection of tiles $\{t_n : n \in \mathbb{Z}^+\}$ so that $\bigcup_{t\in T} \text{supp } t = \mathbb{R}^2$ and $\text{int}(\text{supp } t_i) \cap \text{int}(\text{supp } t_j) = \emptyset$ whenever $i \neq j$.

**Lemma 4.3.** *[12, Theorem 1.4] Any primitive substitution induces a tessellation of the plane.*

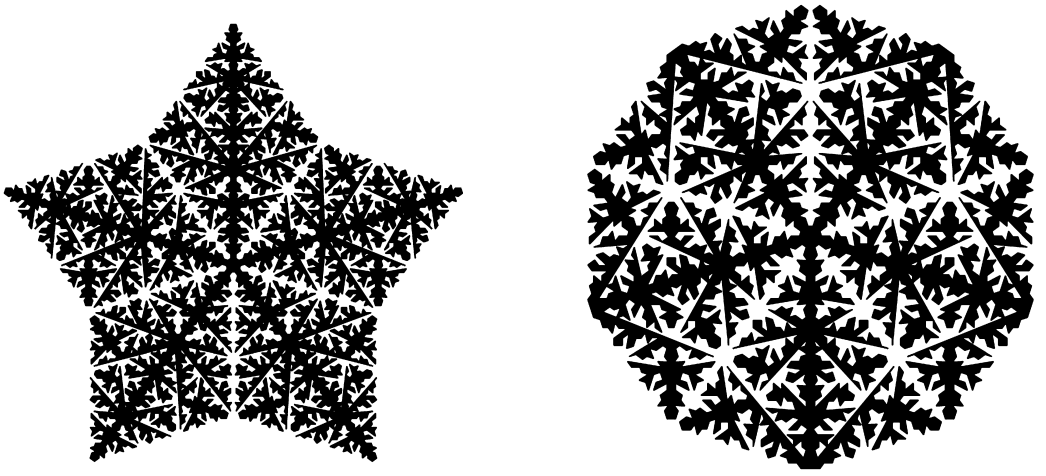

**Fig. 43.** 6th approximants of $F_{star}$ and $F_{deca}$, from left to right.

**Proof.** Assume that $\omega : \mathcal{P} \mapsto \mathcal{P}^*$ is a primitive substitution. Let $p \in \mathcal{P}$ be given. There exists $n \in \mathbb{Z}^+$ and $x \in \mathbb{R}^2$ such that $\{p + x\} \subseteq \omega^n(p + x)$ and $\text{supp } p + x \cap \partial\text{supp } (\omega^n(p + x)) = \emptyset$. That is, a translation of $p$ appears 'inside' of the patch $\omega^n(p + x)$. Hence,

$$\{p + x\} \subseteq \omega^n(p + x) \subseteq \omega^{2.n}(p + x) \subseteq \omega^{3.n}(p + x) \subseteq \dots$$

is an infinite sequence of nested patches such that $\bigcup_{i=1}^{\infty} \omega^{i.n}(p + x)$ is a tessellation of the plane. □

We use the same idea to produce fractal-like relatively dense sets in the plane.

*A relatively dense set in* $\mathbb{R}^2$ Consider the iterative rule shown in Fig. 44. There are three types of tiles up to rotation; a rectangle with side lengths $\sqrt{3}$ and 4, an equilateral triangle with side length $\sqrt{3}$, and an 12-gon with alternatingly aligned side lengths $\sqrt{3}$, 1 and equal internal angles (150°). Observe that iteration of a rectangle tile contains a copy of itself at its centre. This induces a nested collection of patches as depicted in Fig. 45. Nested patches expand in every direction in the plane as iterated, and thereby limit of their supports gives rise to a relatively dense set in the plane. We denote the generated relatively dense set by $H_{eq}$.

**Corollary 4.4.** *The set* $H_{eq}$ *is relatively dense in* $\mathbb{R}^2$.

Notice that patches appearing in iteration steps of the triangle tile given in Fig. 46 are scaled versions of odd-indexed approximants of $F_{eq}^{B^+}$ shown in Fig. 24. Similarly, patches appearing in iteration steps of the rectangle tile given in Fig. 45 are scaled and rotated versions of odd-indexed approximants of $F_{eq}^{A}$ shown in Fig. 28. In particular, iterative construction of $H_{eq}$ is analogue to construction of (rotated version of) $F_{eq}^{A}$.

The set $H_{eq}$ contains only three types of tiles up to rotation and translation. It has a fractal-like feature in the sense that it is constructed through nested sequence of patches, each of which is a collection of tiles that are congruent copy of either of the three tiles. Next, we generalise this construction.

**Proposition 4.5.** *Let* $\omega : \mathcal{P} \mapsto \mathcal{P}^*$ *be a given substitution defined over a finite collection* $\mathcal{P}$ *with an expansion factor* $\lambda > 1$ *such that* $\max\{diam(t) : t \in \lambda^{-n}\omega^n(p),\ p \in \mathcal{P}\} \downarrow 0$ *as* $n \to \infty$, *where* $diam(t)$ *is the diameter of* $\text{supp } t$. *Suppose* $F : [0, 1] \mapsto \text{supp } p$ *is a Lebesgue-type space-filling curve generated by the method explained in Theorem 3.1 and fills* $\text{supp } p$ *for some* $p \in \mathcal{P}$. *Assume that* $F(0) = F(1)$ *and* $\{F_n : n \in \mathbb{Z}^+\}$ *is the*

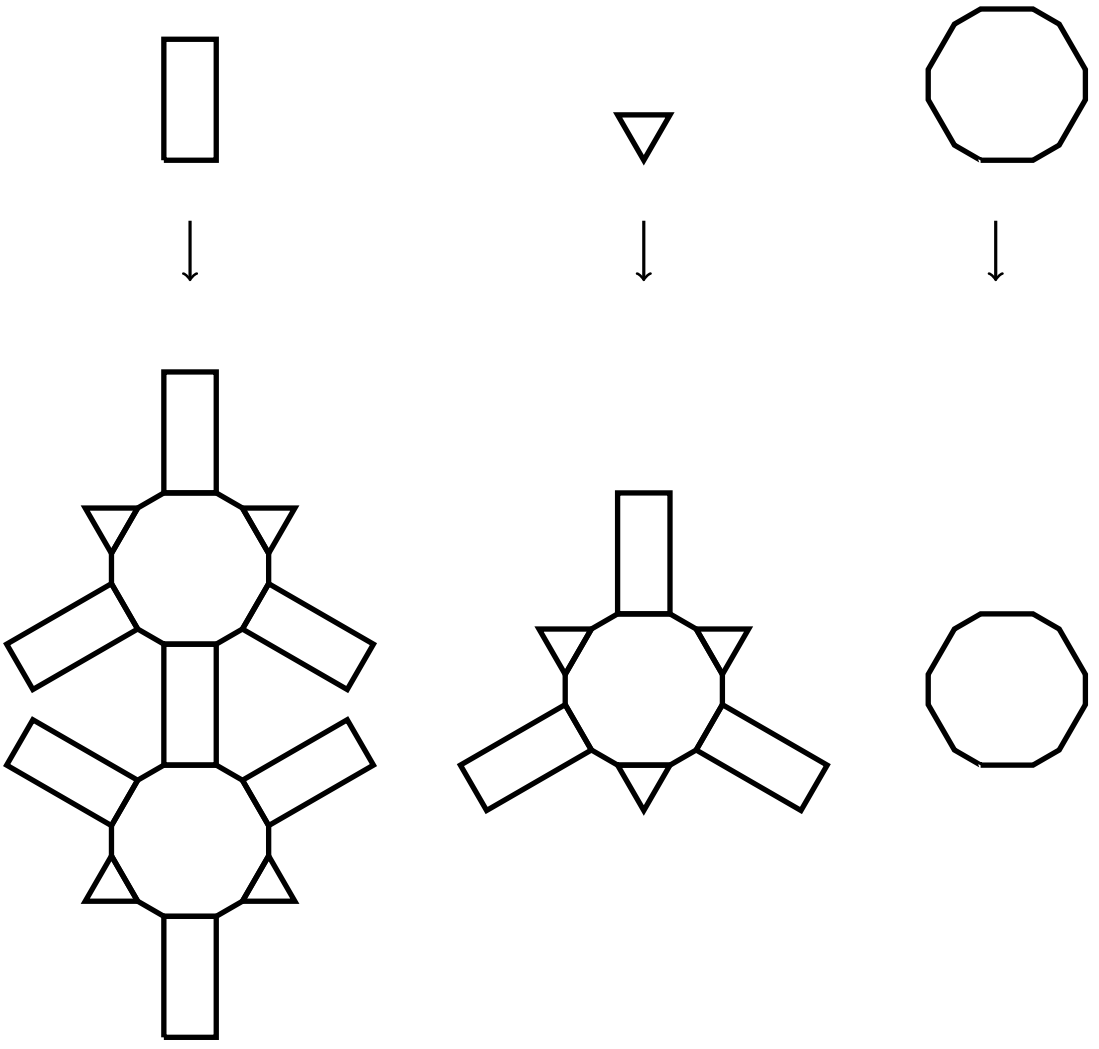

**Fig. 44.** An iteration rule for $H_{eq}$.

*collection of approximants of $F$ (defined on $\lambda^{-n}\omega^n(p)$) generated by filling the associated closed regions (i.e. $F_n$'s are sets in $\mathbb{R}^2$). Assume further there exists $x \in \mathbb{R}^2$ and $k \in \mathbb{Z}^+$ so that*

(1) $p + x \in \omega^k(p + x)$ *and* $\text{supp } (p + x) \cap \partial\text{supp } \omega^k(p + x) = \emptyset$,
(2) $F_1 + x \subseteq \lambda^k(F_{k+1} + x)$ *(i.e. a copy of $F_1$ appears in scaled version of $F_{k+1}$),*
(3) $F_n$ *visits two (scaled) tiles in $\lambda^{-n}\omega^n(p)$ subsequently only if they share a common edge, for every $n \in \mathbb{Z}^+$.*

*Then*

i. $F_{n.k+1} + x \subseteq \lambda^n(F_{(n+1)k+1} + x)$ *for every $n \in \mathbb{Z}^+$.*
ii. $F = \bigcup_{n=0}^{\infty} \lambda^{n.k}(F_{n.k+1} + x)$ *is a relatively dense set in the plane.*
iii. $F$ *can be partitioned into collection of sets $\{A_m : m \in \mathbb{Z}^+\}$ so that there are only finitely many different sets in the collection (up to translation and rotation). Precisely,*
   (a) $\bigcup_m A_m = F$,
   (b) $int(A_i) \cap int(A_j) = \emptyset$ *whenever $i \neq j$, where $int(A_i), int(A_j)$ are interiors of $A_i$ and $A_j$, respectively,*

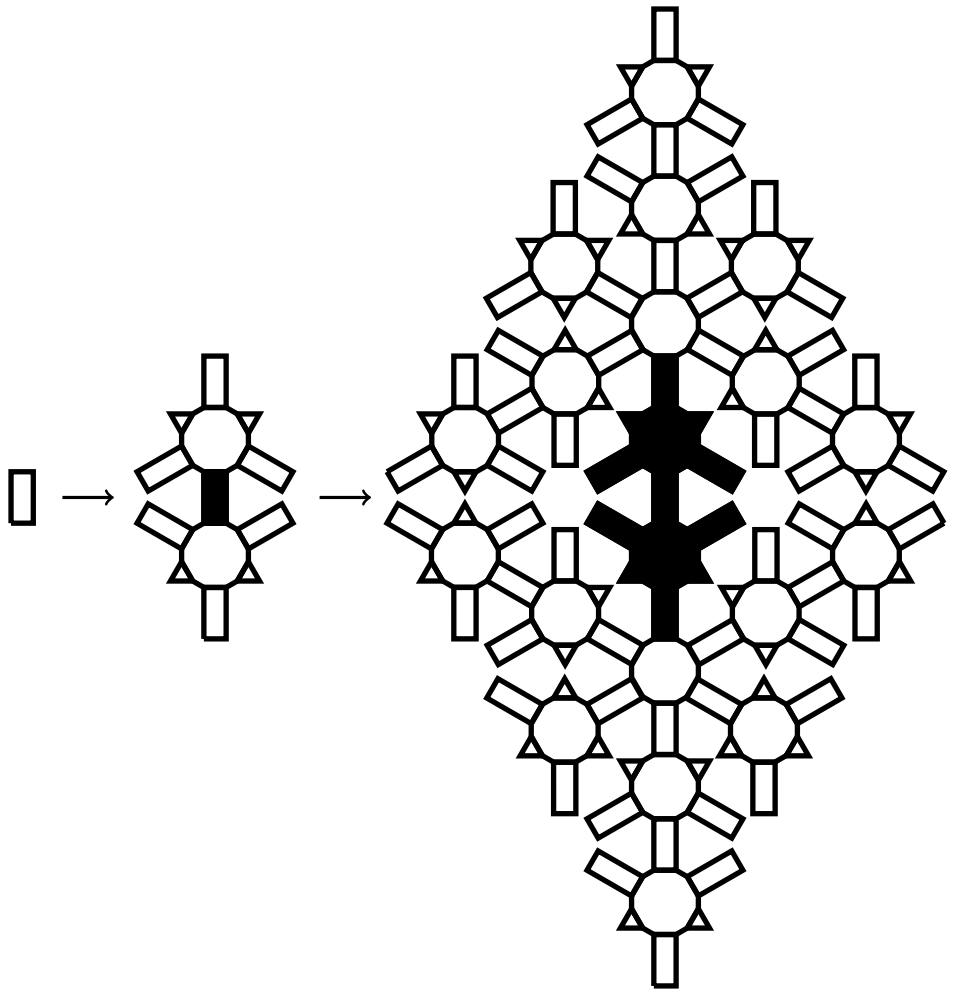

**Fig. 45.** An iterative construction of $H_{eq}$.

(c) *There are finite number of indices* $m_1, \dots m_s \in \mathbb{Z}^+$ *for some* $s \in \mathbb{Z}^+$ *such that for each* $m \in \mathbb{Z}^+$ *there exists* $r_m \in \{m_1, \dots, m_s\}$ *and* $x_m \in \mathbb{R}^2$ *with* $A_m = A_{r_m} + x_m$.

**Proof.** i. We get $\{p+x\} \subseteq \omega^n(p+x) \subseteq \omega^{2n}(p+x) \subseteq \dots$, by (1). So, we can conclude by (2) that

$$F_1 + x \subseteq \lambda^n(F_{n+1} + x) \subseteq \lambda^{2n}(F_{2n+1} + x) \subseteq \lambda^{3n}(F_{3n+1} + x) \subseteq \dots.$$

ii. We have that the collection $T = \bigcup_{i=1} \omega^{in}(p+x)$ is a covering of the plane by (1), using the argument provided in the proof of Lemma 4.3. Note that $F = \bigcup_{i=0}^{\infty} \lambda^{in}(F_{in+1} + x)$ visits every tile in $T$. Thus, $F$ is relatively dense in $\mathbb{R}^2$ because there are only finite different tiles in $\mathcal{P}$.

iii. For each $t \in T$, define $A_t = F \cap \text{supp } t$. Then $F = \bigcup_{t \in T} A_t$. Furthermore, $int(A_{t_i}) \cap int(A_{t_j}) = \emptyset$ whenever $t_i \neq t_j$, where $int(A_{t_i}), int(A_{t_j})$ are interiors of $A_{t_i}, A_{t_j}$, respectively. By (3) and the fact that $|\mathcal{P}|$ is finite, there are only finitely many indices $t_1, \dots, t_m$ for some $m \in \mathbb{Z}^+$ such that for each $t \in T$, there exists $s_t \in \{t_1, \dots, t_m\}$ and $x_t \in \mathbb{R}^2$ with $A_t = A_{s_t} + x_t$. □

**Remark 4.6.** Condition *iii*-(*c*) in Proposition 4.5 is analogue to definition of fractals by Mandelbrot [7]. In particular, condition *iii*-(*c*) assures that there are only finite number of dissections of $F$, whose collection

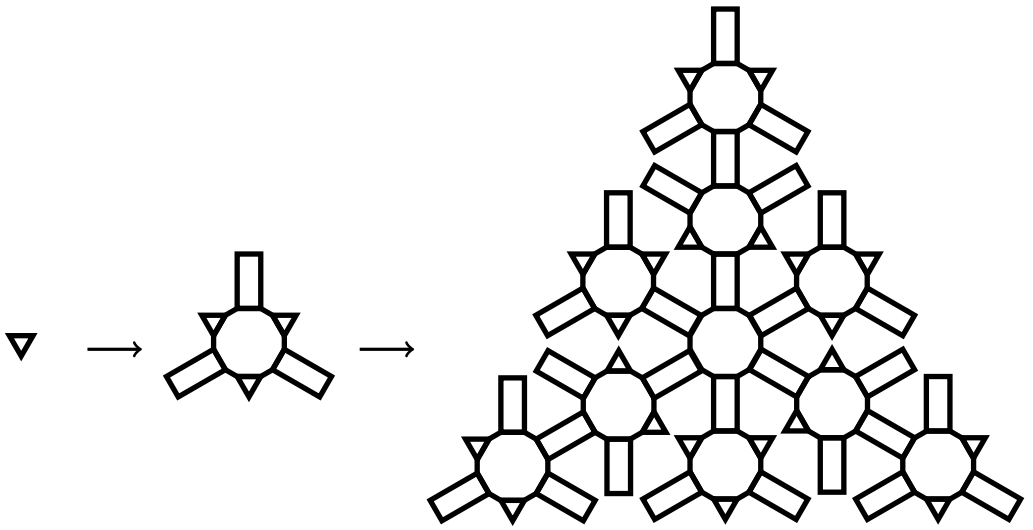

**Fig. 46.** Iteration process of the triangle tile in Fig. 44.

is denoted by $\mathcal{P}$ (analogue to tile set $\mathcal{P}$), such that $F$ can be written as a countable union of sets, each of which is a translational copy of the defined dissections of $F$ (i.e. each of which is a congruent copy of a tile in $\mathcal{P}$).

## Rights retention statement



## Declaration of competing interest

The author states that there is no conflict of interest.

## Acknowledgments

This work was supported by the Ministry of National Education of Turkey. The author would like to thank anonymous reviewers for their helpful comments and suggestion about Bratteli-Vershik systems.

## References

[1] O. Bratteli, Inductive limits of finite-dimensional C*–algebras, Trans. Am. Math. Soc. 171 (1972) 195–234.
[2] G. Cantor, Ein Beitrag zur Mannigfaltigkeitslehre, Crelle J. 84 (1878) 242–258.
[3] D. Frettlöh, E. Harriss, F. Gähler, Tilings encyclopedia, https://tilings.math.uni-bielefeld.de/.
[4] R.H. Herman, I. Putnam, C.F. Skau, Ordered Bratteli diagrams, dimension groups and topological dynamics, Int. J. Math. 3 (1992) 827–864.
[5] D. Hilbert, Über die stetige Abbildung einer Linie auf ein Flächenstück, Math. Ann. 38 (1891) 459–460.
[6] H. Lebesgue, Leçons sur l'Intégration et la Recherche des Fonctions Primitives, Gauthier-Villars, Paris, 1904, pp. 44–45.
[7] B.B. Mandelbrot, The Fractal Geometry of Nature, Macmillan, 1983.
[8] E.H. Moore, On certain crinkly curves, Trans. Am. Math. Soc. 1 (1900) 72–90.
[9] E. Netto, Beitrag zur Mannigfaltigkeitslehre, Crelle J. 86 (1879) 263–268.
[10] G. Peano, Sur une courbe qui remplit toute une aire plane, Math. Ann. 36 (1890) 157–160.
[11] G. Pólya, Über eine Peanosche Kurve, Bull. Acad. Sci. Cracov. (Sci. Math. Nat. Sér. A) 1 (9) (1913).
[12] L. Sadun, Topology of Tiling Spaces, American Mathematical Society, 2008.
[13] H. Sagan, Approximating polygons for Lebesgue's and Schoenberg's space-filling curves, Am. Math. Mon. 93 (5) (1986) 361–368.
[14] H. Sagan, A geometrization of Lebesgue's space-filling curve, Math. Intell. 15 (4) (1993) 37–43.

[15] H. Sagan, Space-Filling Curves, Springer-Verlag, Berlin Heidelberg New York, 1994.
[16] W. Sierpiński, Sur une nouvelle courbe continue qui remplit toute une aire plane, Bull. Acad. Sci. Cracov. (Sci. Math. Nat. Sér. A) 462 (478) (1912).
[17] A.M. Vershik, A theorem on the Markov periodical approximation in ergodic theory, J. Sov. Math. 28 (1985) 667–674.
[18] A.M. Vershik, A.N. Livschits, Adic models of ergodic transformations, spectral theory, substitutions, and related topics, in: Representation Theory and Dynamical Systems, in: Adv. Soviet Math., vol. 9, 1992, pp. 185–205.
[19] W. Wunderlich, Über Peano-Kurven, Elem. Math. 28 (1973) 1–10.